INFORMATION AND CONTROL 5, 279–323 (1962)

Sampling and Reconstruction of Wave-Number-Limited Functions in N-Dimensional Euclidean Spaces*

DANIEL P. PETERSEN†

Weather System Center, United Aircraft Corporation, East Hartford, Connecticut

AND

DAVID MIDDLETON‡

Consulting Physicist, 23 Park Lane, Concord, Massachusetts

The well-known Whittaker-Kotel'nikov-Shannon sampling theorem for frequency-bandlimited functions of time is extended to functions of multidimensional arguments. It is shown that a function whose spectrum is restricted to a finite region of wave-number space may be reconstructed from its samples taken over a periodic lattice having suitably small repetition vectors. The most efficient lattice (i.e., requiring minimum sampling points per unit hypervolume) is not in general rectangular, nor is a unique reconstruction function associated with a given sampling lattice.

The above results also apply to homogeneous wave-number-limited stochastic processes in the sense of a vanishing mean-square error. It is also found that, given a particular sampling lattice, the optimum (mean-square) presampling filter for nonwave-number-limited processes effects an ideal wave-number cutoff appropriate to the specified sampling lattice.

Particular attention is paid to isotropic processes: minimum sam-

---

* This paper includes some preliminary results of research conducted by Mr. Petersen under the guidance of Dr. Middleton, in partial fulfillment of the requirements for the degree Doctor of Engineering Science at Rensselaer Polytechnic Institute.

† Daniel P. Petersen is a candidate for D.E.S., Rensselaer Polytechnic Inst., Hartford Graduate Center, East Windsor Hill, Conn.

‡ David Middleton is Adjunct Professor of Communication Theory and Applied Physics, Rensselaer Polytechnic Inst., Hartford Graduate Center, East Windsor Hill, Conn.

pling lattices are specified up to eight-dimensional spaces, and a number of typical reconstruction functions are calculated.

LIST OF SYMBOLS

$\mathbf{x}$ An N-dimensional vector $(x_1, x_2, \cdots, x_N)$ in sampling space X

X The N-dimensional Euclidean space over which the sampled functions $f(\mathbf{x})$ are defined

$f(\mathbf{x})$ A scalar function of the vector argument $\mathbf{x}$

$\boldsymbol{\omega}$ An N-dimensional vector $(\omega_1, \omega_2, \cdots, \omega_N)$ in wave-number space Ω

$F(\boldsymbol{\omega})$ A scalar function of $\boldsymbol{\omega}$, the Fourier transform of $f(\mathbf{x})$

Ω The N-dimensional Euclidean space over which the spectra $F(\boldsymbol{\omega})$ are defined

B The limiting magnitude of $\frac{\boldsymbol{\omega}}{2\pi}$ for which $F(\boldsymbol{\omega})$ is nonvanishing

$\{\mathbf{v}_j\}$ A set of N vectors forming a basis for X

$\{\mathbf{u}_k\}$ A set of N vectors forming a basis for Ω

$\delta(\mathbf{x})$ The N-dimensional Dirac delta function:

$$\int_\Lambda \delta(\mathbf{x})\, d\mathbf{x} = \begin{cases} 1, & \text{if } \Lambda \text{ contains the origin} \\ 0, & \text{if } \Lambda \text{ does not contain the origin} \end{cases}$$

$\sum_{[l]}$ An N-fold summation: $\sum_{l_1=-\infty}^{\infty} \sum_{l_2=-\infty}^{\infty} \cdots \sum_{l_N=-\infty}^{\infty}$

$\int_X d\mathbf{x}$ An N-fold integration: $\int_{-\infty}^{\infty} \cdots \int_{-\infty}^{\infty} dx_1\, dx_2 \cdots dx_N$

$\mathfrak{R}$ The region of Ω over which $F(\boldsymbol{\omega})$ is nonvanishing

B The parallelepiped in X whose edges are the vectors $\{\mathbf{v}_j\}$

Q The hypervolume of the parallelepiped B

$\boldsymbol{\omega}\cdot\mathbf{x}$ The inner or dot product of the vectors $\boldsymbol{\omega}$ and $\mathbf{x}$:

$$\boldsymbol{\omega}\cdot\mathbf{x} = \omega_1 x_1 + \omega_2 x_2 + \cdots + \omega_N x_N$$

δ_{ij} Kronecker's delta: $\delta_{ij} = 1,\ i = j;\ \delta_{ij} = 0,\ i \neq j$

$\delta_{[m]}^{[l]}$ N-fold Kronecker delta, $\delta_{l_1 m_1}\, \delta_{l_2 m_2} \cdots \delta_{l_N m_N}$

η Sampling efficiency

$E\{\ \}$ The expectation (over the ensemble) of the quantity in brackets, defined over X

$K(\mathbf{x}, \mathbf{y})$ The covariance function $E\{f(\mathbf{x})f(\mathbf{y})\}$ of the random process $f(\mathbf{x})$, with $\mathrm{E}\{f(\mathbf{x})\} = 0$

$\Phi(\boldsymbol{\omega})$ The spectral density function of the process, the Fourier transform of $K(\mathbf{x})$

$f^*(\mathbf{x})$ An estimate of $f(\mathbf{x})$

$\overline{E\{\ \}}$	The uniform average over X of the expectation of a quantity defined on X
$J_{N/2}$	Bessel function of the first kind of order $N/2$
Q_N	The hypervolume of the optimum N-dimensional isotropic sampling lattice cell
A_N	The coefficient of r^N in the formula for hyperspherical volume
$\Delta(\mathbf{x})$	A lattice of Dirac impulses in X
$C_{[m]}$	An expansion coefficient of Nth order, $C_{m_1 m_2 \cdots m_N}$
$\mathbf{Q}$	An $N \times N$ matrix
$\det \mathbf{Q}$	The determinant of $\mathbf{Q}$
$\tilde{\mathbf{Q}}$	The transpose of $\mathbf{Q}$
$\mathbf{I}$	The identity matrix
$[\alpha_{ij}]$	A matrix of elements α_{11}, α_{12}, etc.
R	The hypervolume of the region $\mathcal{R}$ in Ω
P	The hypervolume of the parallelepiped whose edges are the vectors $\{\mathbf{u}_i\}$
$\mathcal{S}$	The class of wave-number-limited functions

I. INTRODUCTION

An expanding segment of engineering activity is today directed toward the development of systems of information collection, processing, dissemination, decision, and control. In the most interesting of these applications, the information so handled is derived in whole or in part from measurements of continuous[1] physical processes which generate uncertainty at an infinite rate. The system design, however, is inevitably constrained by finite precision of instrumentation, finite capacity of communication channels, finite speed and storage capability of processing equipment. Subject to specified or self-imposed technical and budgetary limitations, the designer must select the "best" (in some sense) combination of components and facilities to approximate the desired results.

For monitoring of continuous data sources in the time domain, discrete periodic sampling has become a standard technique. A large body of literature has been devoted to the problems introduced by sampling

[1] Although in the limit natural phenomena may well vary in discrete quantized steps, practical engineering measurements to which sampling theory is applicable are invariably many orders of magnitude coarser than the elementary quantization and may justifiably be considered as operating upon a mathematical continuum.

in feedback control systems (Ragazzini and Franklin, 1958, and bibliography therein), while another, almost disconnected, area of study has been concerned with the information content of sampled data with applications to coding and decoding schemes (Shannon and Weaver, 1949; Jagerman and Fogel, 1956; Fogel, 1955; Elias, 1955; Helms and Thomas, 1962; Linden and Abramson, 1960). Both of these approaches depend upon the intuitive as well as theoretical notion of a process spectrum which tends toward zero at high frequencies—the observed fact that, in all physical systems, only relatively small changes occur in small increments of time. It is natural, then, to idealize this concept mathematically to that of strict spectrum cutoff at a finite frequency, and to examine the implications of such a postulate in terms of the information-generating capability of the process. In spite of the artificiality of the assumed conditions, useful insight is obtained which serves in establishing bounds on performance and first approximations in iterative design procedures.

Fruitful as this concept has been to the communication specialist, its restriction thus far to one-dimensional (i.e., time) processes has prevented application to other areas where physical phenomena must be measured in a multidimensional (space-and-time) continuum. Conspicuous here are the fields of meteorology, oceanography, seismology, acoustics, optics, and radar. Extension of the one-dimensional sampling theory and its associated techniques of data manipulation to multidimensional spaces is an essential step in the development of adequate tools for the analysis and synthesis of information systems in these important fields.

II. BACKGROUND

Whittaker (1915), Nyquist (1928), Kotel'nikov (1933), Shannon (1949), and others have considered the problem of interpolation of band-limited functions. Shannon (1949), for example, used the following argument. Suppose $f(t)$, $-\infty < t < \infty$, is a function whose Fourier transform exists,

$$F(\omega) = \int_{-\infty}^{\infty} f(\tau) e^{-i\omega\tau}\, d\tau, \quad -\infty < \omega < \infty, \quad (1)$$

and that $F(\omega)$ vanishes for $|\omega| > 2\pi B$. The spectrum $F(\omega)$ may, within the passband, be expanded in Fourier series,

$$F(\omega) = \sum_{-\infty}^{\infty} a_k e^{-ik\omega/2B}, \tag{2}$$

where

$$a_k = \frac{1}{4\pi B} \int_{-2\pi B}^{2\pi B} F(\omega) e^{ik\omega/2B}\, d\omega. \tag{3}$$

But the inverse Fourier transform is

$$f(t) = \frac{1}{2\pi} \int_{-\infty}^{\infty} F(\omega) e^{i\omega t}\, d\omega = \frac{1}{2\pi} \int_{-2\pi B}^{2\pi B} F(\omega) e^{i\omega t}\, d\omega, \tag{4}$$

the last step being essential to eliminate the harmonics introduced in the frequency domain by the Fourier expansion. Thus, comparing (3) and (4), we find

$$a_k = \frac{1}{2B} f\left(\frac{k}{2B}\right), \tag{5}$$

and therefore

$$F(\omega) = \frac{1}{2B} \sum_{-\infty}^{\infty} f\left(\frac{k}{2B}\right) e^{-ik\omega/2B}, \tag{6}$$

from which

$$\begin{aligned} f(t) &= \frac{1}{2B} \sum_{-\infty}^{\infty} f\left(\frac{k}{2B}\right) \left\{ \frac{1}{2\pi} \int_{-2\pi B}^{2\pi B} e^{i\omega[t-(k/2B)]}\, d\omega \right\} \\ &= \sum_{-\infty}^{\infty} f\left(\frac{k}{2B}\right) \frac{\sin 2\pi B[t - (k/2B)]}{2\pi B[t - (k/2B)]}. \end{aligned} \tag{7}$$

Equation (7) is the "cardinal" interpolation formula for reconstruction of a continuous function $f(t)$ from a denumerably infinite set of sample values $f(k/2B)$ with the weighting function

$$g(\tau) = \frac{\sin 2\pi B\tau}{2\pi B\tau}. \tag{8}$$

A more general approach has been taken by Middleton (1960) and others which provides considerable insight into the one-dimensional problem and is important for the extension to higher ordered spaces. Suppose we postulate at the outset an interpolation formula based on periodic sampling,

$$f(t) = \sum_{-\infty}^{\infty} f(t_k)g(t - t_k), \tag{9}$$

and assume both $f(t)$ and $g(t)$ are Fourier transformable. We may then consider the sampling as generated by impulse modulation,

$$f(t) = \sum_{-\infty}^{\infty} g(t - t_k) \int_{-\infty}^{\infty} f(\tau)\delta(\tau - t_k)\, d\tau, \tag{10}$$

and invert the order of summation and integration:

$$f(t) = \int_{-\infty}^{\infty} f(\tau)g(t - \tau) \sum_{-\infty}^{\infty} \delta(\tau - t_k)\, d\tau. \tag{11}$$

We next expand the impulse train in Fourier series,

$$\sum_{-\infty}^{\infty} \delta(\tau - t_k) = \frac{1}{T} \sum_{-\infty}^{\infty} e^{-2\pi ik\tau/T}, \tag{12}$$

where $t_k = kT$. Equation (11) is now recognized as a sum of convolutions of the functions

$$\frac{g(t)}{T} \quad \text{and} \quad f(t)e^{-2\pi ikt/T}.$$

Its Fourier transform is the product summation

$$F(\omega) = \frac{G(\omega)}{T} \sum_{-\infty}^{\infty} F\left(\omega + \frac{2\pi k}{T}\right). \tag{13}$$

Equation (13) exhibits the well-known phenomenon of "spectrum repetition" introduced by the sampling procedure (Fig. 1a). It will be an identity for *any* spectral function $F(\omega)$ limited to the same band $|\omega| < 2\pi B$ if and only if

$$T \leqq \frac{1}{2B}$$

and

$$G(\omega) = \begin{cases} T, & |\omega| < 2\pi B \\ 0, & \dfrac{2\pi k}{T} - 2\pi B \leqq |\omega| \leqq \dfrac{2\pi k}{T} + 2\pi B \quad (k = 1, 2, \cdots) \end{cases}. \tag{14}$$

Now if the sampling period is chosen as large as possible (i.e., $T =$

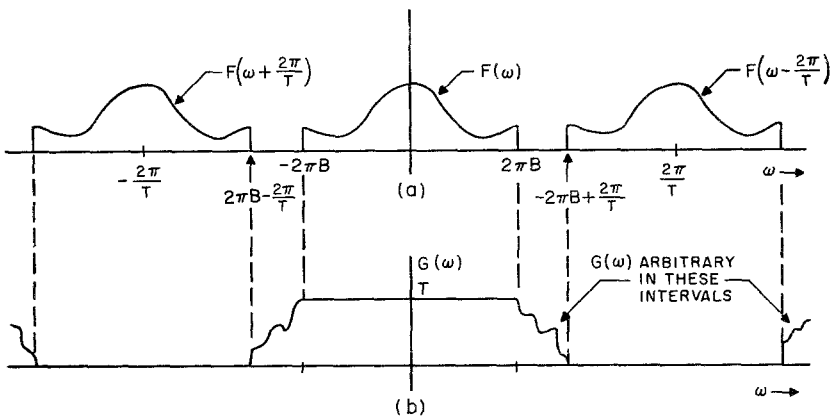

FIG. 1. Spectrum periodicity of a sampled bandlimited function and spectrum of reconstruction function.

$1/2B$), there is only *one* choice for $G(\omega)$ and therefore for $g(t)$:

$$\begin{aligned} g(t) &= \frac{1}{2\pi}\int_{-2\pi B}^{2\pi B}\frac{1}{2B}\,e^{i\omega t}\,d\omega \\ &= \frac{\sin 2\pi Bt}{2\pi Bt}, \end{aligned} \tag{15}$$

as before. However, if the function is sampled faster than necessary, the spectrum $G(\omega)$ of the weighting function $g(t)$ is arbitrary for

$$\frac{2\pi k}{T} + 2\pi B < |\,\omega\,| < \frac{2\pi(k+1)}{T} - 2\pi B, \quad k = 0, 1, 2, \cdots,$$

(Fig. 1b). For example, let $G(\omega) = 0$ in these intervals. We then have

$$\begin{aligned} g(t) &= \frac{1}{2\pi}\int_{-2\pi B}^{2\pi B} Te^{i\omega t}\,d\omega \\ &= \frac{T}{\pi t}\sin 2\pi Bt. \end{aligned} \tag{16}$$

Function (16) no longer exhibits the "orthogonality" property of (8) and (15),[2] and thus implies a linear dependence among the sample values $g(kT)$. In one dimension there is, of course, no advantage in such overly-rapid sampling. We shall see presently, however, that a certain

[2] Namely, $g(0) = 1$ and $g(kT) = g(k/2B) = 0$, $k = \pm 1, \pm 2, \cdots$.

degree of arbitrariness is an *essential* feature of multidimensional sampling and may in some situations be put to definite advantage.

With the exception of Brillouin (1956), who discussed briefly the problems of three-dimensional sampling with particular reference to crystallographic research, little attention appears to have been paid in the literature to multidimensional sampling theory. However, a significant contribution was made in this area by Miyakawa (1959), in a paper not apparently available in a formal English translation. Miyakawa, using an extension of Shannon's (1949) approach, obtained a formula for the N-dimensional "canonical" sampling function and enunciated the inverse relationship between the sampling lattice and the periodicity of the sampled wave-number spectrum. He also gave examples of several two- and three-dimensional sampling lattices and compared their efficiencies with reference to isotropic functions. K. Sasakawa (1960, 1961) published four papers concerning applications of Miyakawa's work; these are not yet available to the authors. Bracewell (1956) discussed sampling and reconstruction (smoothing) of continuous fields but limited his analysis to two dimensions and rectangular lattices.

The present paper, while incidentally making available Miyakawa's important work to American readers, makes the following new contributions:

1. The theory of multidimensional sampling is derived using the delta-modulation approach, thereby sharpening the statement of the theorem and providing a clearer insight into the general sampling problem;

2. The general technique for achieving a minimum sampling lattice is defined;

3. Formal derivations of critical properties of sampling lattices and reconstruction functions are presented;

4. Sampling of isotropic functions is connected with the geometrical problem of close-packed hyperspheres, thus allowing minimum sampling lattices to be specified explicitly up to eighth-order Euclidean spaces;

5. The results are extended to wave-number-limited stochastic processes and to optimum prefiltering and reconstruction of nonwave-number-limited processes; and

6. A number of examples are presented, including in particular the calculation of reconstruction functions for isotropic processes.

III. THE SAMPLING THEOREM IN EUCLIDEAN N-SPACE

We consider a set of (real) functions $\{f(\mathbf{x})\} = \{f(x_1, x_2, \cdots, x_N)\}$ defined over N-dimensional Euclidean space of infinite extent, whose Fourier transforms (Sneddon, 1951) exist:

$$F(\omega) = F(\omega_1, \omega_2, \cdots, \omega_N) = \int_X f(\mathbf{x}) e^{-i\boldsymbol{\omega}\cdot\mathbf{x}} \, d\mathbf{x}. \tag{17}$$

We call the subset $\mathcal{S}$ of such functions "wave-number-limited" if the Fourier transform of every member of $\mathcal{S}$ vanishes outside a finite subspace $\mathcal{R}$ of the "wave-number space" Ω. (Fig. 2). We do not require at this point that $\mathcal{R}$ be symmetrical in any way, or even that it be connected, but only that it lie within a bounded region of Ω. We desire to expand a member function of the set $\mathcal{S}$ in a series of terms whose coefficients are the values of the function at a set of periodic sampling points. To do this, we define the "periodic basis" of the space X as the set of vectors

$$\{\mathbf{v}_j\} = \{\mathbf{v}_1, \mathbf{v}_2, \cdots, \mathbf{v}_N\} \tag{18}$$

and state that the sampling lattice points are all vectors

$$\begin{aligned} \mathbf{v}_{[l]} &= l_1\mathbf{v}_1 + l_2\mathbf{v}_2 + \cdots + l_N\mathbf{v}_N, \\ l_1, l_2, \cdots, l_N &= 0, \pm 1, \pm 2, \cdots. \end{aligned} \tag{19}$$

Thus, we seek a suitable "reconstruction function" $g(\mathbf{x})$ such that $f(\mathbf{x})$ may be expanded as a linear function of its samples:

$$f(\mathbf{x}) = \sum_{[l]} f(\mathbf{v}_{[l]}) g(\mathbf{x} - \mathbf{v}_{[l]}). \tag{20}$$

As in the one-dimensional procedure following (9), let us convert the right side of (20) into a convolution using an N-dimensional Dirac delta-function:

$$f(\mathbf{v}_{[l]}) g(\mathbf{x} - \mathbf{v}_{[l]}) = \int_X f(\boldsymbol{\varrho}) g(\mathbf{x} - \boldsymbol{\varrho}) \delta(\boldsymbol{\varrho} - \mathbf{v}_{[l]}) \, d\boldsymbol{\varrho}. \tag{21}$$

It is now necessary to convert the series of delta-functions into an N-dimensional Fourier series; using the results of Appendix A, we obtain

$$f(\mathbf{x}) = \sum_{[m]} \int_X f(\boldsymbol{\varrho}) e^{-i\boldsymbol{\varrho}\cdot\mathbf{u}_{[m]}} \frac{g(\mathbf{x} - \boldsymbol{\varrho})}{Q} \, d\boldsymbol{\varrho}, \tag{22}$$

where Q is the hypervolume of the parallelepiped formed by the vectors

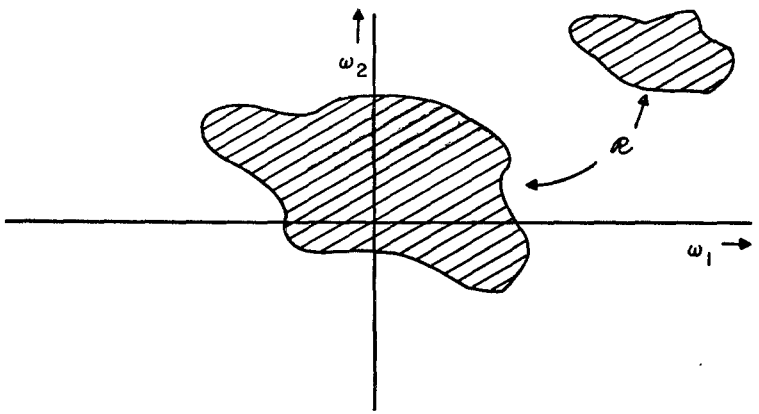

FIG. 2. A limited spectrum in two-dimensional wave-number space

$\{\mathbf{v}_j\}$, and where the vectors $\{\mathbf{u}_k\}$ bear a reciprocal relation to the vectors $\{\mathbf{v}_j\}$, namely,

$$\mathbf{v}_j \cdot \mathbf{u}_k = 2\pi\delta_{jk}\,, \tag{23}$$

δ_{jk} being Kronecker's delta:

$$\delta_{jk} = \begin{cases} 1, & j = k \\ 0, & j \neq k \end{cases}. \tag{24}$$

The integral in (22) is now recognized as a convolution (Sneddon, 1951), so that, taking the Fourier transform of both sides, we get directly

$$F(\boldsymbol{\omega}) = \frac{G(\boldsymbol{\omega})}{Q} \sum_{[m]} F(\boldsymbol{\omega} + \mathbf{u}_{[m]}). \tag{25}$$

We remark here that $F(\boldsymbol{\omega})$ is the Fourier transform of a function $f(\mathbf{x})$ which is unknown except for its membership in the class $\mathcal{S}$ whose spectra are limited to the region $\mathcal{R}$ of wave-number space. What we thus seek is a *universal* function $g(\mathbf{x})$ which will reproduce *any* function of the class $\mathcal{S}$ from its discrete samples. From examination of (25) we see that two conditions must hold to make it an identity:

1. The vectors $\{\mathbf{u}_k\}$ must be large enough and so oriented that adjacent repetitive spectra $F(\boldsymbol{\omega} + \mathbf{u}_{[m]})$ do not overlap; and

2. The spectrum $G(\boldsymbol{\omega})$ of the reconstruction function $g(\mathbf{x})$ must equal the constant Q over the region $\mathcal{R}$ of wave-number space in which

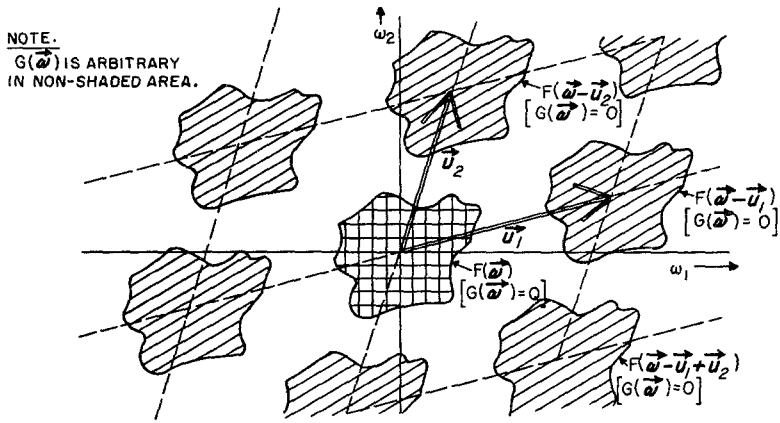

FIG. 3. Two-dimensional spectrum periodicity

$F(\boldsymbol{\omega})$ is nonvanishing, and must equal zero wherever the repetitive spectra $F(\boldsymbol{\omega} + \mathbf{u}_{[m]})$, $\mathbf{u}_{[m]} \neq \mathbf{0}$, are nonvanishing. Its value is arbitrary over that portion of the space Ω, if any, not covered by $F(\boldsymbol{\omega})$ and its periodic images. Figure 3 illustrates these conditions for a two-dimensional function. We note that what was the (avoidable) exception in the one-dimensional problem has become the general rule in multiple dimensions: there now exists in general some interstitial space in which the spectrum of the sampling function $g(\mathbf{x})$ is arbitrary, even though the closest nonoverlapping packing of the repetitive spectra of the sampled function $f(\mathbf{x})$ has been selected.

We have thus established the *N-dimensional sampling theorem*:
A function $f(\mathbf{x})$ *whose Fourier transform* $F(\boldsymbol{\omega})$ *vanishes over all but a finite portion of wave-number space can be everywhere reproduced from its sample values taken over a lattice of points* $\{l_1\mathbf{v}_1 + l_2\mathbf{v}_2 + \cdots + l_N\mathbf{v}_N\}$, $l_1, l_2, \cdots, l_N = 0, \pm 1, \pm 2, \cdots$, *provided that the vectors* $\{\mathbf{v}_j\}$ *are small enough to ensure nonoverlapping of the spectrum* $F(\boldsymbol{\omega})$ *with its images on a periodic lattice defined by the vectors* $\{\mathbf{u}_k\}$, *with* $\mathbf{v}_j \cdot \mathbf{u}_k = 2\pi\delta_{jk}$.

IV. EFFICIENT (MINIMUM) SAMPLING LATTICES

We define an *efficient sampling lattice* as one which uses a minimum number of sampling points to achieve exact reproduction of a wave-number-limited function. We note from Appendix A that the parallelepiped of hypervolume Q, defined by the sampling lattice vectors $\{\mathbf{v}_j\}$, contains one and only one sampling point; thus, $1/Q$ sampling points

are required per unit hypervolume of the space X. Now it may easily be shown (Appendix B) that the hypervolume P of the parallelepiped in wave-number space associated with the vectors $\{\mathbf{u}_k\}$ is $(2\pi)^N/Q$. The sampling efficiency may thus be defined as the ratio

$$\eta = \frac{R}{P} = \frac{RQ}{(2\pi)^N}, \tag{26}$$

where R is the hypervolume of the region $\mathcal{R}$ (e.g., Fig. 2) within which $F(\boldsymbol{\omega})$ is nonvanishing. For highest efficiency we thus seek to enclose $\mathcal{R}$ in the smallest "cell" of wave-number space which is repeatable without overlap on some vector lattice $\{\mathbf{u}_k\}$.

It is important to note here that a parallelepiped is not the only repetitive figure with the vectors $\{\mathbf{u}_k\}$ as a basis. In fact, an infinite variety of spectra may be exactly reproduced under a given sampling plan. Figure 4 illustrates four two-dimensional spectra occupying differently shaped (shaded) areas of the wave-number plane. Since these areas are all repetitive without overlap on the vector basis $(\mathbf{u}_1, \mathbf{u}_2)$, the corresponding functions may all be sampled (with 100% efficiency) on identical lattices defined by the vectors $(\mathbf{v}_1, \mathbf{v}_2)$ inverse to $(\mathbf{u}_1, \mathbf{u}_2)$. The corresponding reconstruction functions would, of course, all be different (Section VIII, A).

Except where the spectral functions occupy analytically describable regions (e.g., hypercubes, parallelepipeds, hyperspheres), the selection of the optimum vector set $\{\mathbf{u}_k\}$ would seem to be a trial-and-error procedure. It is, of course, difficult to conceive of a physical process whose spectrum might exhibit a meaningfully odd shape; moreover, in a practical engineering application, one would have to weigh the disadvantages of inefficient sampling against those of instrumenting a complicated reconstruction function.

Concerning the important class of functions having isotropic spectra, however, we can be more definite. We define "isotropic" here in the broad sense as describing a spectrum which cuts off at the same wave-number magnitude in all directions, i.e., whose region $\mathcal{R}$ is a hypersphere. Thus, the question of the most efficient sampling lattices for N-dimensional isotropic processes is connected with the geometrical problem of the closest packing of hyperspheres. Coxeter (1951) has defined the lattices of centers of close-packed spheres up to eight-dimensional spaces. In Appendix C we derive the corresponding sampling lattices and compare their efficiencies with those of simple hypercubic lattices. In particular, it is seen that a 120° rhombic lattice in two dimensions, and

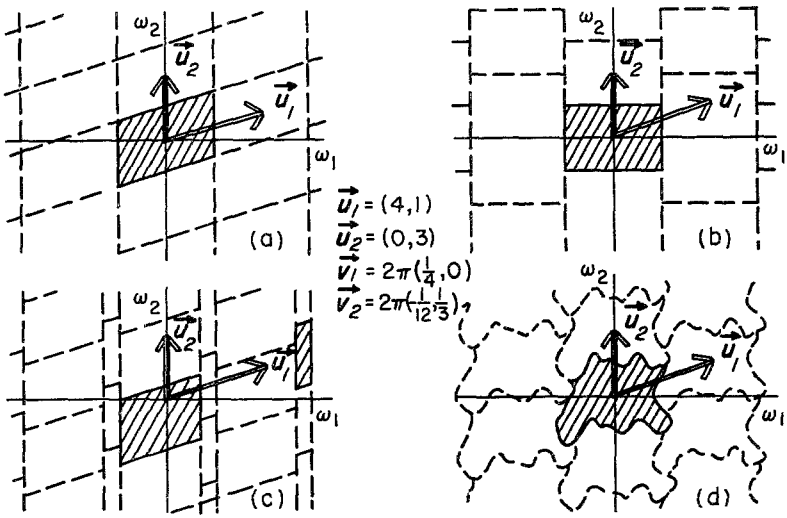

FIG. 4. Spectra of functions reproduced by identical sampling lattices

a "body-centered cubic" lattice in three dimensions, are significantly more efficient than simple square and cubic lattices respectively.

V. WEIGHTING OR RECONSTRUCTION FUNCTIONS

From condition 2, Section III, it is evident that the weighting or reconstruction function

$$g(\mathbf{x}) = \frac{1}{(2\pi)^N} \int_\Omega G(\boldsymbol{\omega}) e^{i\boldsymbol{\omega}\cdot\mathbf{x}}\, d\boldsymbol{\omega} \tag{27}$$

is not uniquely determined by the spectrum of the sampled function or by the selection of a sampling lattice. Its form, in fact, depends on the value chosen for it in the "interstitial" regions of wave-number space (Fig. 3). If, however, we choose $G_c(\boldsymbol{\omega})$ *to be constant* $(=Q)$ *over one complete repeatable cell in wave-number space and vanish elsewhere*, then the associated $g_c(\mathbf{x})$ will be denoted the "canonical" weighting function for the particular spectrum and sampling plan. It is demonstrated in Appendix D that such canonical functions are *orthogonal* over the space X, which also implies that

$$g_c(\mathbf{v}_{[l]}) = \begin{cases} 1, & l_1 = l_2 = \cdots = l_N = 0 \\ 0, & l_1, l_2, \cdots, l_N = 0, \pm 1, \pm 2, \cdots \\ & (\text{except } l_1 = l_2 = \cdots = l_N = 0) \end{cases}, \tag{28}$$

a property which guarantees linear independence of sample values. A number of examples of canonical weighting functions are given in Section VIII; in one dimension we have, of course, the well-known "cardinal" function (15).

A remark on the significance of orthogonal weighting functions as applied to sampling theory seems in order here. We note first that orthogonal functions are frequently sought as elements of series expansions because of the invaluable property that coefficients may be calculated independently rather than through solution of simultaneous equations. In the Karhunen-Loève expansion (Davenport and Root, 1958), we stipulate further that the coefficients be uncorrelated. Neither of these features applies here, however; in sampling theory we *postulate* that the coefficients of the expansion be the sampled values themselves; they *are* independently measurable and, if correlated in the original process, they *must* remain so. For reconstruction, we must use the series for all points except the sample points themselves; here we use the measured values regardless of the orthogonality of the weighting function. It seems probable that convergence of the series *near sampling points* is more rapid using orthogonal functions; it is not clear that the *average* convergence (over the space X) is necessarily better.

From (26) and (27) it is seen that the sampling efficiency η is numerically equal to $g(\mathbf{0})$ if $G(\boldsymbol{\omega})$ is made to vanish outside of $\mathcal{R}$. The efficiency η is thus also a measure of the "local autonomy" of sample points.

For isotropic processes, a weighting function whose spectrum is constant up to the wave-number limit in all directions (i.e., over the hypersphere), although not orthogonal for $N > 1$, has the advantage of considerable simplicity compared with the corresponding canonical function. This is demonstrated in the examples of Section VIII.

VI. WAVE-NUMBER-LIMITED STOCHASTIC PROCESSES

We now turn our attention to the sampling of stochastic processes in Euclidean N-space. As in the one-dimensional theory, we no longer consider individual functions $f(\mathbf{x})$ and their amplitude spectra $F(\boldsymbol{\omega})$, but the statistical (in particular, second-moment) properties of an ensemble $\{f(\mathbf{x})\}$. We assume in the usual way that the process is wide-sense homogeneous ("stationary") and has zero mean value (with obvious modifications in the event of nonzero mean), so that the ensemble average covariance may be expressed as a function of a single (vector) argument:

$$K(\mathbf{x}, \mathbf{y}) = E\{f(\mathbf{x})f(\mathbf{y})\} = K(\mathbf{x} - \mathbf{y}) = K(\mathbf{z}), \tag{29}$$

whose Fourier transform, the process spectral intensity density function $\Phi(\boldsymbol{\omega})$, exists, except possibly for isolated delta-function singularities:

$$\Phi(\boldsymbol{\omega}) = \int_X K(\mathbf{x}) e^{-i\boldsymbol{\omega}\cdot\mathbf{x}} d\mathbf{x}. \tag{30}$$

We seek a weighting function $g(\mathbf{x})$ that will provide an optimum estimate $f^*(\mathbf{x})$, under a least-mean-square-error criterion, of the process representation $f(\mathbf{x})$ based on a linear combination of its periodic samples:

$$f^*(\mathbf{x}) = \sum_{[l]} f(\mathbf{v}_{[l]}) g(\mathbf{x} - \mathbf{v}_{[l]}). \tag{31}$$

Having found this optimum function $g(\mathbf{x})$ in the general case, we will then wish to examine the conditions, if any, under which the mean-square error at every point $\mathbf{x}$ may vanish. In analogy with the one-dimensional situation (Balakrishnan, 1957), we expect this to be achievable when, and only when, the process is wave-number-limited. Accordingly, using (29) and (31) to expand the mean-square error, we obtain

$$\begin{aligned} E\{[f(\mathbf{x}) - f^*(\mathbf{x})]^2\} &= K(\mathbf{0}) - 2\sum_{[l]} K(\mathbf{x} - \mathbf{v}_{[l]}) g(\mathbf{x} - \mathbf{v}_{[l]}) \\ &\quad + \sum_{[l]} \sum_{[m]} K(\mathbf{v}_{[l]} - \mathbf{v}_{[m]}) g(\mathbf{x} - \mathbf{v}_{[l]}) g(\mathbf{x} - \mathbf{v}_{[m]}). \end{aligned} \tag{32}$$

We note at this point that the expected error (over the ensemble) is, in general, a function of $\mathbf{x}$. Furthermore, the minimization of (32) may be carried out independently for each value of $\mathbf{x}$ within a basic sampling cell (i.e., the parallelepiped formed by the vectors $\{\mathbf{v}_j\}$), since for each such value of $\mathbf{x}$ we need choose only a denumerable set of weighting values $\{g(\mathbf{x} - \mathbf{v}_{[l]})\}$. As has been remarked in the one-dimensional case (Stewart, 1956), the optimum function must ensure zero error at the sampling points themselves.

We proceed now in the usual way by assuming an arbitrary variation $\epsilon h(\mathbf{x})$ of $g(\mathbf{x})$ and equating to zero the derivative of the expected error with respect to ϵ at $\epsilon = 0$, taking advantage where appropriate of the homogeneity of the process and the evenness of $K(\mathbf{x})$. We obtain thus the relation

$$\sum_{[l]} K(\mathbf{v}_{[l]}) g(\mathbf{x} - \mathbf{v}_{[l]}) = K(\mathbf{x}). \tag{33}$$

Equation (33) reveals that the optimum reconstruction function $g(\mathbf{x})$ for the *process* $\{f(\mathbf{x})\}$ is one which exactly reproduces the *nonrandom* covariance function $K(\mathbf{x})$ from its samples. Assuming that its Fourier transform $G(\boldsymbol{\omega})$ exists and proceeding exactly as in Section III, we obtain the wave-number relation

$$\Phi(\boldsymbol{\omega}) = \frac{G(\boldsymbol{\omega})}{Q} \sum_{[m]} \Phi(\boldsymbol{\omega} + \mathbf{u}_{[m]}). \tag{34}$$

Now since $\Phi(\boldsymbol{\omega})$ was assumed known a priori, (34) specifies $G(\boldsymbol{\omega})$ uniquely for all values of $\boldsymbol{\omega}$ for which the summation on the right is nonvanishing.[3] Also, since $K(\mathbf{x})$ is real and even, $\Phi(\boldsymbol{\omega})$, $G(\boldsymbol{\omega})$, and $g(\mathbf{x})$ are all real and even. *We note particularly that so far no assumption of wave-number limiting has been made.*

Substituting (33) into (32), we find for the minimum mean-square error

$$E\{[f(\mathbf{x}) - f^*(\mathbf{x})]^2\} = K(\mathbf{0}) - \sum_{[l]} K(\mathbf{x} - \mathbf{v}_{[l]}) g(\mathbf{x} - \mathbf{v}_{[l]}). \tag{35}$$

The error may be expressed in the wave-number domain by expanding the summation on the right of (35) in terms of delta functions and using an N-dimensional version of Parseval's theorem (Morse and Feshbach, 1953):

$$E\{[f(\mathbf{x}) - f^*(\mathbf{x})]^2\} = \frac{1}{(2\pi)^N} \cdot \int_\Omega \left[\Phi(\boldsymbol{\omega}) - \frac{G(\boldsymbol{\omega})}{Q} \sum_{[l]} e^{-i\mathbf{x}\cdot\mathbf{u}_{[l]}} \Phi(\boldsymbol{\omega} + \mathbf{u}_{[l]}) \right] d\boldsymbol{\omega}. \tag{36}$$

By substituting (34) in (36) and observing relation (23), we note that, as expected, *the mean square error vanishes at all sampling lattice points* $\mathbf{x} = \mathbf{v}_{[m]}$. *But for the integral to vanish for all* $\mathbf{x}$, *it is necessary that* $\Phi(\boldsymbol{\omega})$ *vanish outside a basic cell in wave-number space, while* $G(\boldsymbol{\omega})$ *must equal* Q *where* $\Phi(\boldsymbol{\omega})$ *is nonzero and must equal zero where the repetitive images* $\Phi(\boldsymbol{\omega} + \mathbf{u}_{[l]})$ *are nonzero.* This is, of course, the same condition that ensures exact reproduction of N-dimensional deterministic functions, as developed in Section III. We again point out that, in deriving these results for wave-number-limited stochastic processes, we have incidentally also obtained the optimum filter equation (34) and expressions (35) and (36) for the mean-square error of optimally filtered nonwave-number-limited N-dimensional stochastic processes.

[3] If $\sum_{[m]} \Phi(\boldsymbol{\omega} + \mathbf{u}_{[m]})$ is everywhere nonvanishing, we can easily show, analogously to Stewart (1956), that $g(\mathbf{x})$ must be orthogonal, i.e., must satisfy condition (28). If $\sum_{[m]} \Phi(\boldsymbol{\omega} + \mathbf{u}_{[m]})$ vanishes anywhere [implying, since the spectral density is nonnegative, that $\Phi(\boldsymbol{\omega})$ must also vanish], then (34) may be satisfied for arbitrary $G(\boldsymbol{\omega})$ at those points, and $g(\mathbf{x})$ need not be orthogonal.

Since, as stated previously, the reconstruction function $g(\mathbf{x})$ minimizes the mean-square error independently at every point $\mathbf{x}$, the error remains a minimum when averaged with any weighting penalty over an elementary sampling cell. A quantity of considerable interest, and also one which yields convenient expressions, is the mean-square error *uniformly* averaged over a sampling cell B:

$$\overline{E\{[f(\mathbf{x}) - f^*(\mathbf{x})]^2\}} = K(\mathbf{0}) - \frac{1}{Q}\int_B \sum_{[l]} K(\mathbf{x} - \mathbf{v}_{[l]})g(\mathbf{x} - \mathbf{v}_{[l]})\, d\mathbf{x}. \tag{37}$$

Observing that the integrand is a function of $(\mathbf{x} - \mathbf{v}_{[l]})$, we invert the order of summation and integration, and change the dummy variable:

$$\frac{1}{Q}\sum_{[l]}\int_B K(\mathbf{x} - \mathbf{v}_{[l]})g(\mathbf{x} - \mathbf{v}_{[l]})\, d\mathbf{x} = \frac{1}{Q}\sum_{[l]}\int_{B-\mathbf{v}_{[l]}} K(\mathbf{y})g(\mathbf{y})\, d\mathbf{y}. \tag{38}$$

But the summation of integrals over elementary cells is simply the integral over the entire space X; therefore

$$\overline{E\{[f(\mathbf{x}) - f^*(\mathbf{x})]^2\}} = K(\mathbf{0}) - \frac{1}{Q}\int_X K(\mathbf{x})g(\mathbf{x})\, d\mathbf{x}. \tag{39}$$

Again invoking Parseval's theorem, the expression in the wave-number domain becomes

$$\overline{E\{[f(\mathbf{x}) - f^*(\mathbf{x})]^2\}} = \frac{1}{(2\pi)^N}\int_\Omega \Phi(\boldsymbol{\omega})\left[1 - \frac{G(\boldsymbol{\omega})}{Q}\right] d\boldsymbol{\omega}, \tag{40}$$

and, substituting for $G(\boldsymbol{\omega})$ from (34),

$$\overline{E\{[f(\mathbf{x}) - f^*(\mathbf{x})]^2\}} = \frac{1}{(2\pi)^N}\int_\Omega \Phi(\boldsymbol{\omega})\left[1 - \frac{\Phi(\boldsymbol{\omega})}{\sum_{[m]} \Phi(\boldsymbol{\omega} + \mathbf{u}_{[m]})}\right] d\boldsymbol{\omega}. \tag{41}$$

Expressions (39), (40), and (41), of course, are valid (and nonvanishing) for the general (nonwave-number-limited) situation and vanish for a suitably sampled wave-number-limited process.

VII. OPTIMUM PRESAMPLE FILTERING OF NONWAVE-NUMBER-LIMITED STOCHASTIC PROCESSES

The question now arises, "But suppose the process is not wave-number-limited, but is accessible before sampling. Is there any possible advantage in smoothing or filtering the raw data before sampling?" The

answer is, in general, "Yes." In the one-dimensional case this problem has been considered by Spilker (1960), Chang (1961), DeRusso (1961), and Brown (1961).

Let us suppose then that the sample values $\psi(\mathbf{v}_{[l]})$ have themselves been derived from a linear filtering operation on a representation of the original process $\{f(\mathbf{x})\}$:

$$\psi(\mathbf{v}_{[l]}) = \int_X f(\mathbf{y})\gamma(\mathbf{v}_{[l]} - \mathbf{y})\, d\mathbf{y}. \tag{42}$$

The estimated values $f^*(\mathbf{x})$ are again obtained from a series of weighting functions with the sampled values as coefficients:

$$f^*(\mathbf{x}) = \sum_{[l]} g(\mathbf{x} - \mathbf{v}_{[l]})\psi(\mathbf{v}_{[l]}). \tag{43}$$

Again, we desire to minimize the mean-square error,

$$E\{[f(\mathbf{x}) - f^*(\mathbf{x})]^2\} = K(\mathbf{0}) - 2\sum_{[l]} g(\mathbf{x} - \mathbf{v}_{[l]}) \cdot \int_X K(\mathbf{x} - \mathbf{y})\gamma(\mathbf{v}_{[l]} - \mathbf{y})\, d\mathbf{y} + \sum_{[l]}\sum_{[m]} g(\mathbf{x} - \mathbf{v}_{[l]})g(\mathbf{x} - \mathbf{v}_{[m]}) \cdot \int_X \int_X K(\mathbf{y} - \mathbf{z})\gamma(\mathbf{v}_{[l]} - \mathbf{y})\gamma(\mathbf{v}_{[m]} - \mathbf{z})\, d\mathbf{y}\, d\mathbf{z}. \tag{44}$$

In optimizing the reconstruction function $g(\mathbf{x})$ we may proceed exactly as before, obtaining the defining equation analogous to (33),

$$\sum_{[l]} g(\mathbf{x} - \mathbf{v}_{[l]}) \int_X \int_X K(\mathbf{y} - \mathbf{z})\gamma(-\mathbf{y})\gamma(\mathbf{v}_{[l]} - \mathbf{z})\, d\mathbf{y}\, d\mathbf{z} = \int_X K(\mathbf{x} - \mathbf{y})\gamma(-\mathbf{y})\, d\mathbf{y}. \tag{45}$$

Next converting the left side of (45) into a triple convolution using delta functions, expanding the delta function series into an exponential series, and taking Fourier transforms, we obtain

$$\Phi(\boldsymbol{\omega})\Gamma(-\boldsymbol{\omega}) = \frac{G(\boldsymbol{\omega})}{Q}\sum_{[m]} \Gamma(\boldsymbol{\omega} - \mathbf{u}_{[m]})\Gamma(\mathbf{u}_{[m]} - \boldsymbol{\omega})\Phi(\mathbf{u}_{[m]} - \boldsymbol{\omega}), \tag{46}$$

where $\Gamma(\boldsymbol{\omega})$ is the spectrum of the presample filter function $\gamma(\mathbf{x})$. Equation (46) defines the optimum $G(\boldsymbol{\omega})$ with $\Gamma(\boldsymbol{\omega})$ [and, of course, $\Phi(\boldsymbol{\omega})$] fixed. We must next find the optimum $\Gamma(\boldsymbol{\omega})$ with $G(\boldsymbol{\omega})$ [and $\Phi(\boldsymbol{\omega})$] fixed. We recognize at once that this task is essentially more difficult

since now the minimizations of the mean-square error at different points $\mathbf{x}$ are interdependent. As appropriate in the particular application, we may choose to minimize the error at a specific point $\mathbf{x}$, or a weighted average error over the sampling space X. The equations become quite tractable, however, if we make the reasonable specification of minimum mean-square error *uniformly* averaged over X; or, equivalently (because of homogeneity), over a single basic cell B:

$$\begin{aligned}\overline{E\{[f(\mathbf{x}) - f^*(\mathbf{x})]^2\}} &= K(\mathbf{0}) \\ &\quad - \frac{2}{Q}\int_B \sum_{[l]} g(\mathbf{x} - \mathbf{v}_{[l]}) \int_X K(\mathbf{x} - \mathbf{y})\gamma(\mathbf{v}_{[l]} - \mathbf{y})\, d\mathbf{y}\, d\mathbf{x} \\ &\quad + \frac{1}{Q}\int_B \sum_{[l]}\sum_{[m]} g(\mathbf{x} - \mathbf{v}_{[l]})g(\mathbf{x} - \mathbf{v}_{[m]}) \\ &\qquad \cdot \int_X\int_X K(\mathbf{y} - \mathbf{z})\gamma(\mathbf{v}_{[l]} - \mathbf{y})\gamma(\mathbf{v}_{[m]} - \mathbf{z})\, d\mathbf{y}\, d\mathbf{z}\, d\mathbf{x}.\end{aligned} \tag{47}$$

A change of variables yields

$$\begin{aligned}\overline{E\{[f(\mathbf{x}) - f^*(\mathbf{x})]^2\}} &= K(\mathbf{0}) \\ &\quad - \frac{2}{Q}\int_B \sum_{[l]} g(\mathbf{x} - \mathbf{v}_{[l]}) \int_X K(\mathbf{z})\gamma(\mathbf{v}_{[l]} - \mathbf{x} + \mathbf{z})\, d\mathbf{z}\, d\mathbf{x} \\ &\quad + \frac{1}{Q}\int_B \sum_{[l]}\sum_{[k]} g(\mathbf{x} - \mathbf{v}_{[l]})g(\mathbf{x} - \mathbf{v}_{[l]} - \mathbf{v}_{[k]}) \\ &\qquad \cdot \int_X\int_X K(\boldsymbol{\delta} - \boldsymbol{\tau})\gamma(-\boldsymbol{\delta})\gamma(\mathbf{v}_{[k]} - \boldsymbol{\tau})\, d\boldsymbol{\delta}\, d\boldsymbol{\tau}\, d\mathbf{x}.\end{aligned} \tag{48}$$

Examination of (48) now reveals the integrand over B to be a function of $(\mathbf{x} - \mathbf{v}_{[l]})$. As in the manipulation of (37), (38), and (39), we may therefore eliminate the summation over $[l]$ and integrate $d\mathbf{x}$ over the entire space X:

$$\begin{aligned}\overline{E\{[f(\mathbf{x}) - f^*(\mathbf{x})]^2\}} &= K(\mathbf{0}) - \frac{2}{Q}\int_X g(\mathbf{x}) \\ &\quad \cdot \int_X K(\mathbf{z})\gamma(\mathbf{z} - \mathbf{x})d\mathbf{z}\, d\mathbf{x} + \frac{1}{Q}\int_X \sum_{[k]} g(\mathbf{x})g(\mathbf{x} - \mathbf{v}_{[k]}) \\ &\quad \cdot \int_X\int_X K(\boldsymbol{\delta} - \boldsymbol{\tau})\gamma(-\boldsymbol{\delta})\gamma(\mathbf{v}_{[k]} - \boldsymbol{\tau})\, d\boldsymbol{\delta}\, d\boldsymbol{\tau}\, d\mathbf{x}.\end{aligned} \tag{49}$$

Again converting the summation to a sum of delta-function convolutions and, in turn, to a Fourier series, we obtain

$$\overline{E\{[f(\mathbf{x}) - f^*(\mathbf{x})]^2\}} = K(\mathbf{0}) - \frac{2}{Q}\int_X g(\mathbf{x}) \cdot \int_X K(\mathbf{z})\gamma(\mathbf{z} - \mathbf{x})\, d\mathbf{z}\, d\mathbf{x} + \frac{1}{Q^2}\sum_{[k]}\int_X\int_X g(\mathbf{x})g(\mathbf{x} - \boldsymbol{\varrho}) \cdot \int_X\int_X K(\boldsymbol{\delta} - \boldsymbol{\tau})\gamma(-\boldsymbol{\delta})\gamma(\boldsymbol{\varrho} - \boldsymbol{\tau})e^{-i\boldsymbol{\varrho}\cdot\mathbf{u}_{[k]}}\, d\boldsymbol{\delta}\, d\boldsymbol{\tau}\, d\boldsymbol{\varrho}\, d\mathbf{x}. \tag{50}$$

Now a standard variational procedure applied to $\gamma(\mathbf{x})$ yields the defining integral equation

$$\int_X g(\mathbf{y})K(\mathbf{y} - \mathbf{x})\, d\mathbf{y} = \frac{1}{Q}\sum_{[k]}\int_X\int_X\int_X g(\mathbf{y})g(\mathbf{y} - \boldsymbol{\varrho})K(\mathbf{x} - \mathbf{z})\gamma(\boldsymbol{\varrho} - \mathbf{z})e^{-i\boldsymbol{\varrho}\cdot\mathbf{u}_{[k]}}\, d\boldsymbol{\varrho}\, d\mathbf{z}\, d\mathbf{y}, \tag{51}$$

and, finally, taking Fourier transforms in the usual manner, we have

$$G(\boldsymbol{\omega})\Phi(-\boldsymbol{\omega}) = \frac{1}{Q}\sum_{[k]} G(\boldsymbol{\omega} + \mathbf{u}_{[k]})G(-\boldsymbol{\omega} - \mathbf{u}_{[k]})\Phi(\boldsymbol{\omega})\Gamma(-\boldsymbol{\omega}). \tag{52}$$

Since $\Phi(\boldsymbol{\omega})$ is even, (52) yields an expression for $\Gamma(\boldsymbol{\omega})$ in terms of $G(\boldsymbol{\omega})$ alone. Simultaneous solution of (46) and (52) is now required. This, however, is not a trivial task; we show in Appendix E that, if $\Phi(\boldsymbol{\omega})$ is an arbitrary nonvanishing intensity spectrum, Eqs. (46) and (52) are satisfied if, and only if, $G(\boldsymbol{\omega})\Gamma(\boldsymbol{\omega}) = Q$ within (not necessarily *everywhere* within) a repeatable symmetrical cell of wave-number space, and both $G(\boldsymbol{\omega}) = 0$ and $\Gamma(\boldsymbol{\omega}) = 0$ elsewhere.[4] The equations do not appear to yield information on the optimum *shape* of the basic cell. They are evidently a *necessary* but not a *sufficient* condition, and further investigation is required.

Let us compute the average mean-square error by substituting (51) in (50):

$$\overline{E\{[f(\mathbf{x}) - f^*(\mathbf{x})]^2\}} = K(\mathbf{0}) - \frac{1}{Q}\int_X\int_X g(\mathbf{x})K(\mathbf{x} - \mathbf{y})\gamma(-\mathbf{y})\, d\mathbf{y}\, d\mathbf{x}. \tag{53}$$

[4] Although it is only required to hold their product constant, it would invariably seem convenient to choose both $G(\boldsymbol{\omega})$ and $\Gamma(\boldsymbol{\omega})$ to be individually constant over their common region of coverage. In particular, if $\Gamma(\boldsymbol{\omega}) = 1$ over this region, the resultant field is ideally smoothed and undistorted before sampling.

Again, a Parseval relation allows us to write equivalently

$$\overline{E\{[f(\mathbf{x}) - f^*(\mathbf{x})]^2\}} = \frac{1}{(2\pi)^N}\int_\Omega \Phi(\boldsymbol{\omega})\left[1 - \frac{G(\boldsymbol{\omega})\Gamma(\boldsymbol{\omega})}{Q}\right]d\boldsymbol{\omega}. \quad (54)$$

Now from (54) and Appendix E we observe that the integrand vanishes where $G(\boldsymbol{\omega})\Gamma(\boldsymbol{\omega}) = Q$ and equals $\Phi(\boldsymbol{\omega})$ where $G(\boldsymbol{\omega})$ [and $\Gamma(\boldsymbol{\omega})$] vanish. From this we may immediately conclude that the error will be minimized if, from every denumerable set of arguments $\{\boldsymbol{\omega} + \mathbf{u}_{[k]}\}$ we include within our basic cell that value for which $\Phi(\boldsymbol{\omega})$ is greatest [$\Phi(\boldsymbol{\omega})$ is, of course, nonnegative].[5] $G(\boldsymbol{\omega})$ and $\Gamma(\boldsymbol{\omega})$ will thus cover the *complete* basic cell and, within the constraint of repeatability, the shape of this cell will tend to conform to the iso-intensity contours of the process spectrum. For example, the optimum prefiltering functions for isotropic processes with monotonically decreasing spectra will be the "canonical" functions calculated in Section VIII, C and D. An example of a "narrowband" two-dimensional spectrum and the "passband" (shaded) region of the optimum prefilter spectrum under a given repeatability constraint is shown in Fig. 5.

It is emphasized that the above results apply only to the problem of optimum prefiltering, sampling and reconstruction of nonwave-number-limited stochastic processes under the criterion of minimum mean-square error *uniformly averaged* over an infinite sampling domain. We are led under these conditions to the intuitively reasonable conclusion that, having chosen a particular sampling lattice (or density of sampling points), we have rendered "unobservable" those wave numbers outside a cell of definitely limited extent in wave-number space. The optimum prefiltering operation is then one that eliminates these extraneous wave numbers and avoids the introduction of "aliasing" errors. This result has only recently been stated in the one-dimensional situation (Brown, 1961).

It is evident that, since we were free to obtain simply unity (over the entire space Ω) as the optimum prefilter function spectrum, the combination $G(\boldsymbol{\omega})$ and $\Gamma(\boldsymbol{\omega})$ defined above must yield smaller error than would be possible if no prefilter were used. Whether or not the improvement is significant depends, of course, on the actual process spectrum $\Phi(\boldsymbol{\omega})$; however, useful bounds may be derived. Let us return to Eq. (32) and find the average error over an elementary sampling cell B without,

[5] This can easily be shown in a manner analogous to the one-dimensional proof; *cf.* Davenport and Root (1958), p. 106.

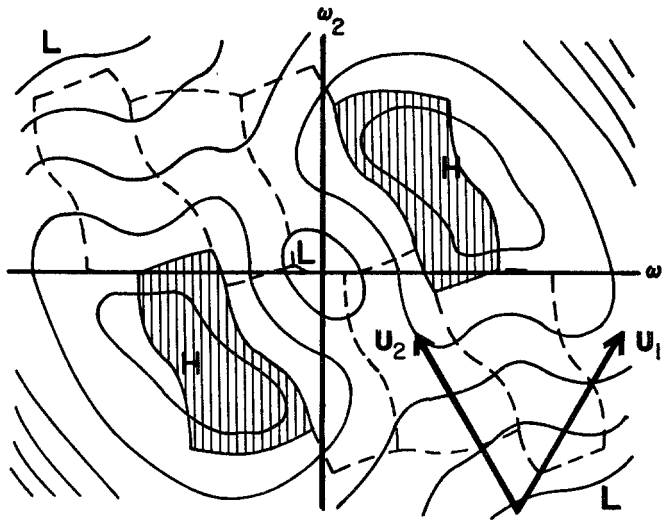

FIG. 5. An optimum prefilter spectrum on the vector basis $\mathbf{u}_1$, $\mathbf{u}_2$, [H = high intensity; L = low intensity]

as yet, specifying the form of the reconstruction function $g(\mathbf{x})$:

$$\overline{E\{[f(\mathbf{x}) - f^*(\mathbf{x})]^2\}} = K(\mathbf{0}) - \frac{2}{Q}\int_B \sum_{[l]} K(\mathbf{x} - \mathbf{v}_{[l]})g(\mathbf{x} - \mathbf{v}_{[l]})\,d\mathbf{x} + \frac{1}{Q}\int_B \sum_{[l]}\sum_{[m]} K(\mathbf{v}_{[l]} - \mathbf{v}_{[m]})g(\mathbf{x} - \mathbf{v}_{[l]})g(\mathbf{x} - \mathbf{v}_{[m]})\,d\mathbf{x}. \tag{55}$$

We again exchange the summation over $[l]$ for integration over the entire space X,

$$\overline{E\{[f(\mathbf{x}) - f^*(\mathbf{x})]^2\}} = K(\mathbf{0}) - \frac{2}{Q}\int_X K(\mathbf{x})g(\mathbf{x})\,d\mathbf{x} + \frac{1}{Q}\int_X \sum_{[k]} K(\mathbf{v}_{[k]})g(\mathbf{x})g(\mathbf{x} + \mathbf{v}_{[k]})\,d\mathbf{x}, \tag{56}$$

convert to a convolution with a Fourier expansion of delta functions,

$$\overline{E\{[f(\mathbf{x}) - f^*(\mathbf{x})]^2\}} = K(\mathbf{0}) - \frac{2}{Q}\int_X K(\mathbf{x})g(\mathbf{x})\,d\mathbf{x} + \frac{1}{Q^2}\sum_{[m]}\int_X\int_X K(\boldsymbol{\varrho})g(\mathbf{x})g(\mathbf{x} + \boldsymbol{\varrho})\,e^{i\boldsymbol{\varrho}\cdot\mathbf{u}_{[m]}}\,d\boldsymbol{\varrho}\,d\mathbf{x}, \tag{57}$$

and transform to the wave-number space Ω:

$$\overline{E\{[f(\mathbf{x}) - f^*(\mathbf{x})]^2\}} = \frac{1}{(2\pi)^N}\int_\Omega \Phi(\omega)\, d\omega - \frac{2}{(2\pi)^N}\int_\Omega \Phi(\omega)\frac{G(-\omega)}{Q}\, d\omega + \frac{1}{(2\pi)^N}\int_\Omega \Phi(\omega)\frac{\sum_{[m]} G(\omega + \mathbf{u}_{[m]})G(-\omega - \mathbf{u}_{[m]})}{Q^2}\, d\omega. \tag{58}$$

We now specify that $G(\omega) = Q$ over the same basic cell defined in the discussion following (54), and $G(\omega) = 0$ elsewhere. Observing from Appendix E that this cell is symmetrical with respect to the origin, we find that the third term on the right of (58) is equal to the first; therefore,

$$\overline{E\{[f(\mathbf{x}) - f^*(\mathbf{x})]^2\}} = \frac{2}{(2\pi)^N}\int_\Omega \Phi(\omega)\left[1 - \frac{G(\omega)}{Q}\right] d\omega. \tag{59}$$

On comparing (59) with (54), we conclude that the average mean-square error of reconstruction using an ideal filter (but no prefilter) is exactly twice the total spectral intensity *outside* the filter "passband," and thus also twice the error obtainable using ideal prefiltering. [In the one-dimensional case, a result equivalent to (59) has also been obtained by Jordan (1960), Zheleznov (1958), and Ignat'ev (1960).] Moreover, (54) and (59) constitute lower and upper bounds respectively on the average mean-square error of reconstruction using an *optimum* filter [cf. (34) and (41)], with no prefilter. This result follows since: (1) the ideal prefilter must yield lower error than any arrangement using postfiltering alone, otherwise the optimum prefilter would be unity over all Ω; (2) the optimum postfilter must yield error no greater than that produced by any *arbitrarily* chosen function, and, a fortiori, the ideal or canonical filter.

VIII. EXAMPLES

In this section a number of specific examples of sampling lattices and reconstruction functions are presented, both to illustrate the theory developed in earlier sections and to support its application to problems of general interest.

A. Alternate Canonical Weighting Functions Associated with a Given Sampling Lattice

It was stated in Section IV that a given sampling lattice might be

associated with many different shapes of spectral region in wave-number space. Figure 4 illustrates four such regions in a two-dimensional space, all associated with identical sampling lattices. The canonical reconstruction functions associated with the regions shown in parts (a), (b), and (c) of the figure are listed below; obviously, the shape shown in part (d) was deliberately made complicated to emphasize the discussion and only a tedious graphical computation would be possible.

$$\text{(a)} \quad g_a(x_1, x_2) = \frac{4 \sin \tfrac{1}{2}(4x_1 + x_2) \sin \tfrac{1}{2}(3x_2)}{3x_2(4x_1 + x_2)} \; ;$$

$$\text{(b)} \quad g_b(x_1, x_2) = \frac{\sin 2x_1 \sin \tfrac{3}{2}x_2}{3x_1 x_2} \; ;$$

$$\text{(c)} \quad g_c(x_1, x_2) = -\frac{4 \sin \tfrac{3}{2}x_2}{3x_2(4x_1 + x_2)} \left[e^{-(i/16)(4x_1+13x_2)} \sin \frac{7}{16}(4x_1 + x_2) + e^{(23i/16)(4x_1+x_2)} \sin \frac{1}{16}(4x_1 + x_2) \right].$$

In each case, we may verify directly that the functions are orthogonal, i.e.,

$$g(0, 0) = 1;$$

$$g\left[\frac{\pi}{6}(3m - n), \frac{2\pi n}{3}\right] = 0, \quad m, n = 0, \pm 1, \pm 2, \cdots, \quad (\text{except } m = n = 0).$$

Note that a nonsymmetrical spectrum yields a complex weighting function, but one that is still orthogonal.

B. Parallelepiped Spectrum Cells

If the wave-number spectrum can be efficiently enclosed within a parallelepiped centered at the origin, then a particularly simple sampling function results. The sampling lattice is also easily determined (but is not unique since successive rows, planes, etc. may be "staggered" any desired amount). In particular, a rectangular grid may always be selected. The two-dimensional case is illustrated in Fig. 6.

The sampling function is the same for all these equivalent lattices, whether successive rows are staggered or not:

$$g(\mathbf{x}) = \frac{Q}{(2\pi)^N} \int_{\mathcal{R}} e^{i\boldsymbol{\omega}\cdot\mathbf{x}} \, d\boldsymbol{\omega}, \tag{60}$$

where $\mathcal{R}$ is defined by the vectors forming its edges, $\{\mathbf{u}_k\}$, ($k = 1, 2,$

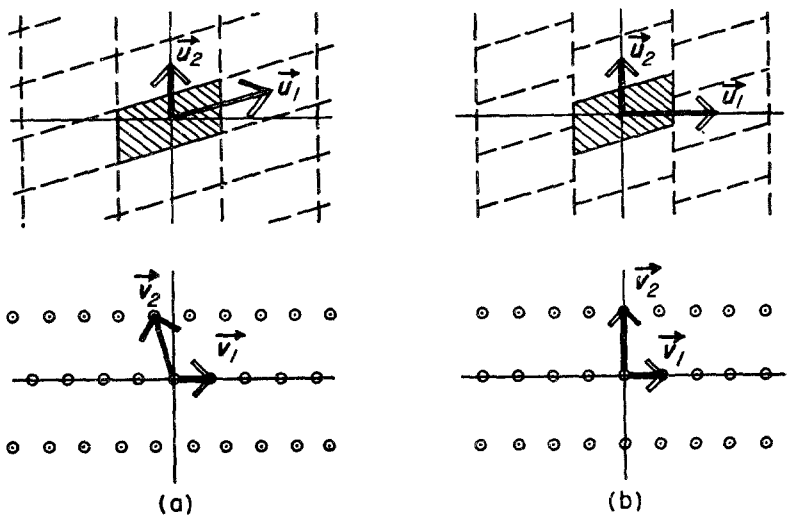

FIG. 6. Alternate arrangements of parallelepiped spectra

$\cdots, N$). Transforming from Ω space to Λ space by the linear relation

$$\omega = \lambda_1 \mathbf{u}_1 + \lambda_2 \mathbf{u}_2 + \cdots + \lambda_N \mathbf{u}_N, \quad -\tfrac{1}{2} \leq \lambda_j < \tfrac{1}{2}, \tag{61}$$

the Jacobian of which is $(2\pi)^N/Q$ (Appendix B), we obtain

$$g(\mathbf{x}) = \int_{-1/2}^{1/2} \cdots \int_{-1/2}^{1/2} \exp[i(\lambda_1 \mathbf{u}_1 \cdot \mathbf{x} + \lambda_2 \mathbf{u}_2 \cdot \mathbf{x} + \cdots + \lambda_N \mathbf{u}_N \cdot \mathbf{x})]\, d\lambda_1 \cdots d\lambda_N$$
$$= \prod_{k=1}^{N} \frac{\sin \tfrac{1}{2}\mathbf{u}_k \cdot \mathbf{x}}{\tfrac{1}{2}\mathbf{u}_k \cdot \mathbf{x}} \,. \tag{62}$$

This function obviously obeys the orthogonality condition in view of the relation (23) between the vectors $\{\mathbf{u}_k\}$ in Ω space and $\{\mathbf{v}_j\}$ in X space.

If, furthermore, the spectrum occupies a rectangular region of wave-number space, so that we may take

$$\mathbf{u}_k = (u_1 \delta_{1k}, u_2 \delta_{2k}, \cdots, u_N \delta_{Nk}), \tag{63}$$

then

$$g(\mathbf{x}) = \prod_{k=1}^{N} \frac{\sin \tfrac{1}{2} u_k x_k}{\tfrac{1}{2} u_k x_k} \,, \tag{64}$$

which is merely a product of one-dimensional "cardinal" functions.

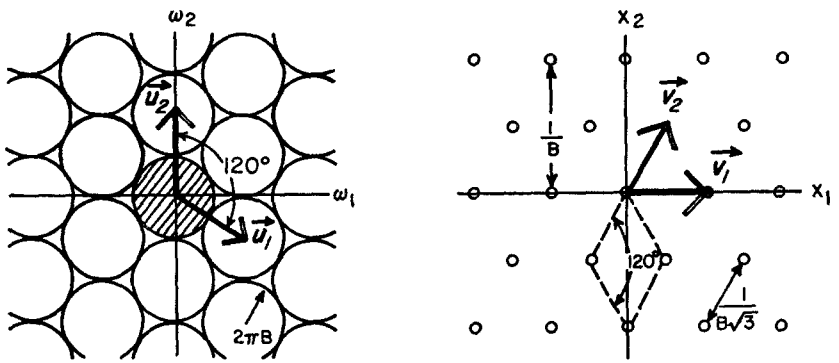

FIG. 7. Optimum sampling lattice for two-dimensional isotropic function

C. TWO-DIMENSIONAL ISOTROPIC FUNCTIONS: CANONICAL WEIGHTING

If the spectrum of a function is bounded by a circle of radius $2\pi B$ in the wave-number plane, Appendix C shows that the unique optimum sampling lattice is the 120° rhombic with spacing of sample points equal to $1/B\sqrt{3}$ (Fig. 7). The efficiency η is 90.8%, to be compared with 78.5% for the largest possible square lattice.

The canonical sampling function for this case is found by taking the inverse transform of a function equal to a constant Q over the interior of a regular hexagon of side $4\pi B/\sqrt{3}$. The constant Q is merely $(2\pi)^2$ times the inverse of the area of the hexagon: $Q = 1/2\sqrt{3}B^2$. Therefore,

$$g_c^{(2)}(\mathbf{x}) = \frac{1}{(2\pi)^2}\frac{1}{2\sqrt{3}B^2}\iint_{\text{Reg. Hex.}} e^{i\boldsymbol{\omega}\cdot\mathbf{x}}\,d\boldsymbol{\omega}; \tag{65}$$

$$g_c^{(2)}(x_1, x_2) = \frac{\begin{array}{l}2x_1\cos(2\pi Bx_1/\sqrt{3})\cos 2\pi Bx_2 - 2x_1\cos(4\pi Bx_1/\sqrt{3}) \\ \quad - 2\sqrt{3}\sin(2\pi Bx_1/\sqrt{3})\sin 2\pi Bx_2\end{array}}{(2\pi B)^2\, x_1(x_1^2 - 3x_2^2)}. \tag{66}$$

It may easily be verified that $g_c^{(2)}(x_1, x_2)$ obeys the orthogonality condition, i.e.,

$$\begin{aligned} g_c^{(2)}(0,0) &= 1; \\ g_c^{(2)}\left(\frac{l-m}{2B\sqrt{3}}, \quad \frac{l+m}{2B}\right) &= 0, \qquad l, m = 0, \pm 1, \pm 2, \cdots, \\ &\qquad\qquad (\text{except } l = m = 0). \end{aligned} \tag{67}$$

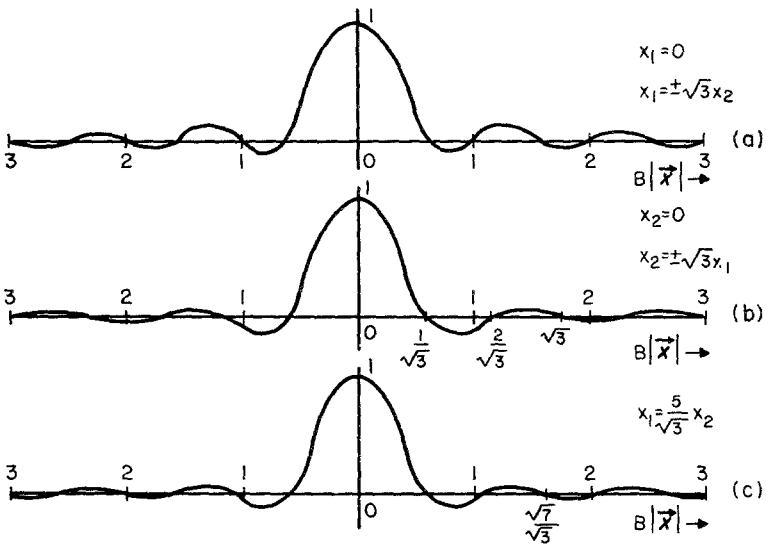

FIG. 8. Variation of canonical two-dimensional weighting function along radial lines.

Figure 8 shows the variation of the weighting function (66) as **x** varies along several lines in the plane. Figure 8(a) is a plot along $x_1 = 0$, or along lines making an angle of $\pm 30°$ with the x_1 axis. Plot 8(b) is along the x_1 axis or lines at $\pm 60°$ angles. Plot 8(c) is along lines whose tangents are $3\sqrt{3}$, $\sqrt{3}/5$, and $\sqrt{3}/2$. On each curve the lower abscissa references locate the actual sampling points intercepted by the chosen trajectory; these of course lie at different distances from the origin in the different directions. It is important to note that, in all cases, the significant weighting effect occurs within the innermost "shell" of sampling points at a radius $1/B\sqrt{3}$.

D. THREE-DIMENSIONAL ISOTROPIC FUNCTIONS: CANONICAL WEIGHTING

Efficient sampling of a three-dimensional isotropic process, wave-number-limited to $2\pi B$ in Ω space, requires a "body-centered cubic" sampling lattice, the cube edge being $1/\sqrt{2}B$ units in length (Appendix C and Fig. 9). The efficiency η is 74.2%, to be compared with 52.3% for the largest simple cubic lattice.

The calculation of canonical sampling functions for isotropic processes

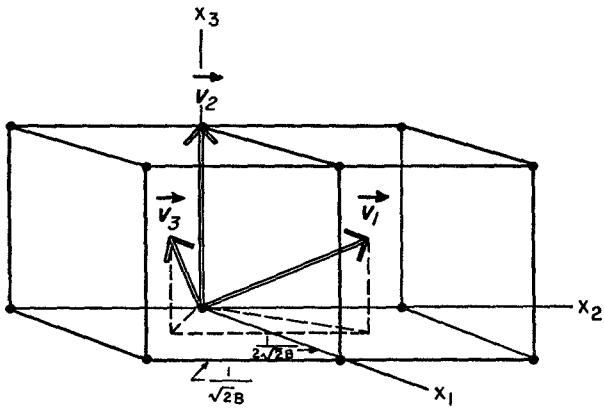

FIG. 9. Body-centered cubic lattice

becomes rapidly more tedious as the dimensionality increases. In three dimensions, it is necessary to integrate a Fourier kernel throughout a regular rhombic dodecahedron of width $4\pi B$ between parallel faces. The result is:

$$g_c^{(3)}(\mathbf{x}) = g_c^{(3)}(x_1, x_2, x_3)$$

$$= \frac{1}{2(\sqrt{2}\pi B)^3[x_1^4 + x_2^4 + x_3^4 - 2(x_1^2x_2^2 + x_1^2x_3^2 + x_2^2x_3^2)]}$$

$$\times \{-2x_1 \sin 2\pi\sqrt{2}\,Bx_1 - 2x_2 \sin 2\pi\sqrt{2}\,Bx_2 - 2x_3 \sin 2\pi\sqrt{2}\,Bx_3$$

$$+ (x_1 + x_2 + x_3) \sin \pi\sqrt{2}\,B(x_1 + x_2 + x_3) \qquad (68)$$

$$+ (x_1 - x_2 + x_3) \sin \pi\sqrt{2}\,B(x_1 - x_2 + x_3)$$

$$+ (x_1 - x_2 - x_3) \sin \pi\sqrt{2}\,B(x_1 - x_2 - x_3)$$

$$+ (x_1 + x_2 - x_3) \sin \pi\sqrt{2}\,B\,(x_1 + x_2 - x_3)\}.$$

Again, it may be verified directly that $g_c^{(3)}\ (0, 0, 0) = 1$, and that, at other sampling points,

$$g_c^{(3)}\left(\frac{p+q-r}{2\sqrt{2}\,B}, \frac{p-q+r}{2\sqrt{2}\,B}, \frac{-p+q+r}{2\sqrt{2}\,B}\right) = 0, \qquad (69)$$

$$p, q, r = 0, \pm 1, \pm 2, \cdots, \text{(except } p = q = r = 0),$$

thus confirming the orthogonality of (68). Figure 10 shows the variation

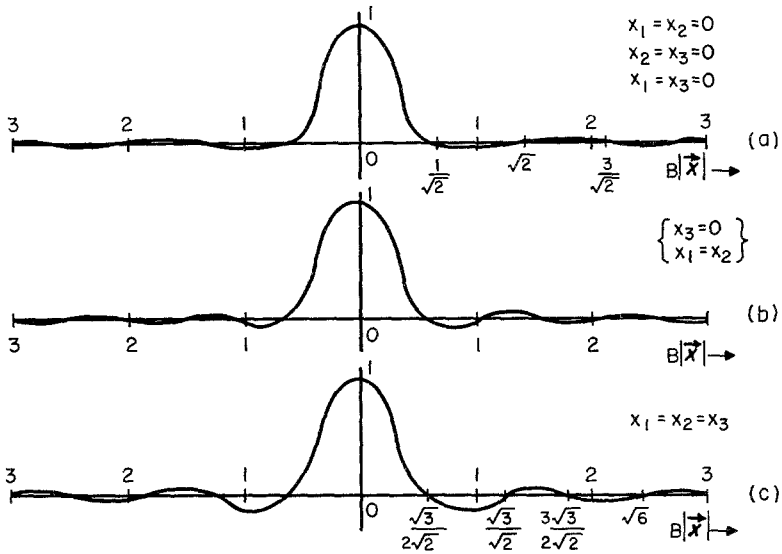

FIG. 10. Variation of canonical three-dimensional weighting function along radial lines.

of $g_c^{(3)}(\mathbf{x})$ as $\mathbf{x}$ varies along several lines in the X space. These one-dimensional functions all have similar shapes near the origin, but their zero crossings occur at different distances from the origin in the various directions, corresponding to the locations of sampling lattice points.

E. Isotropic Weighting Functions

As discussed in Section V, the spectra of weighting functions for isotropically limited processes may be taken as constant only within the hypersphere bounding the process spectrum and not within the complete wave-number cell. Although the resulting functions are not orthogonal, this may have little significance in practical applications, and their simplicity affords definite advantages. In such a case we may write immediately the inverse Fourier transformation

$$g_i^{(N)}(\mathbf{x}) = \frac{1}{(2\pi)^N} Q_N \int_{|\omega|<2\pi B} e^{i\omega \mathbf{x}} \, d\omega, \tag{70}$$

where Q_N is the hypervolume of the N-dimensional isotropic sampling lattice parallelepiped (i.e., the determinant of the $[v_{ji}^{(N)}]$ matrix, cf. Appendices B and C). Now, because of symmetry, we may take $\mathbf{x} =$

$(0, 0, \cdots, x)$ and integrate immediately throughout an $(N - 1)$-dimensional hypersphere:

$$g_i^{(N)}(x) = \frac{1}{(2\pi)^N} Q_N A_{N-1} \int_{-2\pi B}^{2\pi B} [(2\pi B)^2 - \omega^2]^{(N-1)/2} e^{i\omega x} \, d\omega, \quad (71)$$

where A_N is the coefficient of r^N in the formula for N-dimensional spherical volume:

$$A_N = \frac{(\pi)^{N/2}}{\Gamma[(N + 2)/2]}. \quad (72)$$

With the change of variable $\omega = 2\pi B \cos \theta$, (71) may be integrated to yield (Jahnke and Emde, 1945):

$$g_i^{(N)}(x) = \left(\frac{B}{x}\right)^{N/2} Q_N J_{N/2}(2\pi B x). \quad (73)$$

Using the results of Appendix C, we may now write directly the isotropic weighting functions of various orders. For example, in two dimensions, we have

$$g_i^{(2)}(x) = \frac{J_1(2\pi B x)}{2\sqrt{3} B x}. \quad (74)$$

This function is to be compared with the canonical function (66); it is, of course, considerably simpler and has the satisfying property (for isotropic processes) that the influence of sample values depends only on their respective distances from the point to be reconstructed. It is not, on the other hand, orthogonal; it does not vanish at sampling points other than the origin, and its value at $x = 0$ is not unity but 0.908, which as remarked in Section V is numerically equal to the sampling efficiency. Figure 11 shows the variation of $g_i^{(2)}(\mathbf{x})$ as $\mathbf{x}$ varies along any line in the plane; this should be compared with Fig. 8 not only in general shape but in the approximate locations of the zero crossings. Except for a multiplicative factor, the result (74) was also obtained by Bracewell (1956). His formula is correct for *prefiltering* isotropic data, since it omits the factor Q_N.

In three dimensions, instead of the canonical function (68), we have simply

$$\begin{aligned} g_i^{(3)}(x) &= \left(\frac{B}{x}\right)^{3/2} \frac{1}{4\sqrt{2}B^3} J_{3/2}(2\pi B x) \\ &= \frac{\pi}{\sqrt{2}(2\pi B x)^3} [\sin 2\pi B x - 2\pi B x \cos 2\pi B x]. \end{aligned} \quad (75)$$

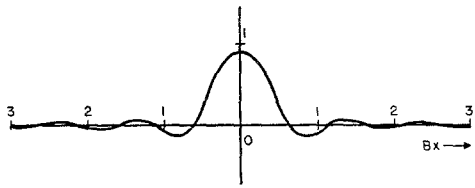

FIG. 11. Variation of isotropic two-dimensional weighting function along a radial line.

We see again that a considerably simpler expression is obtained, especially in the fact that the influence of sample values depends only on their distance from the interpolation point. As may be seen from Fig. 12, a plot of $g_i^{(3)}(x)$ vs. x, the function equals 0.742, not unity, at the origin and does not vanish at other sampling points. The distances of several "shells" of sampling lattice points from the origin are marked for reference on the abscissa of Fig. 12. Again, the weighting is essentially complete within the innermost ' shell" of lattice points.

The fourth-dimensional weighting function, as a matter of interest, is

$$g_i^{(4)}(x) = \left(\frac{B}{x}\right)^2 \frac{1}{8B^4} J_2(2\pi Bx) = \frac{1}{8(Bx)^2} J_2(2\pi Bx). \tag{76}$$

It may easily be determined that $g_i^{(4)}(0) = \pi^2/16 = 0.617$. Figure 13 shows the variation of $g_i^{(4)}(\mathbf{x})$ along a radial line in the four-dimensional space X. The distance of the innermost "shell" of sampling points from the origin is marked on the abscissa for reference.

IX. SUMMARY AND CONCLUSIONS

A general sampling theorem for wave-number-limited processes in N-dimensional Euclidean spaces has been established. This theorem states that a function whose spectrum exists and is nonvanishing over only a finite region of wave-number space may be exactly reproduced from its sample values taken on a periodic lattice with suitably small repetition vectors. Although the theorem is analogous to the well-known Whittaker-Kotel'nikov-Shannon sampling theorem (and reduces to it in the case of single dimensionality), the multidimensional problem exhibits many interesting and unexpected features. Conspicuous among these are the nonuniqueness of sampling plans (even among those of equivalent efficiency) and of reconstruction or weighting functions. A number of examples are presented, both for purposes of illustration and for their practical importance.

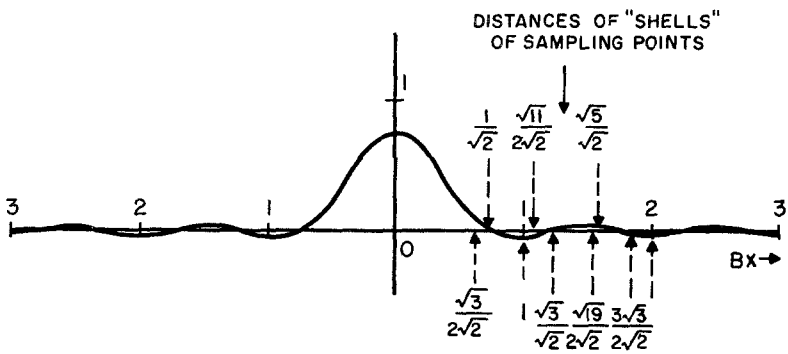

FIG. 12. Variation of isotropic three-dimensional weighting function along a radial line.

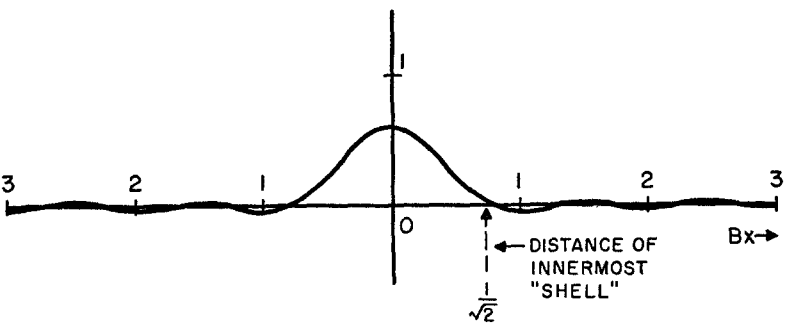

FIG. 13. Variation of isotropic four-dimensional weighting function along a radial line.

The significant topic of isotropic processes has been given particular attention. First, sampling of an N-dimensional isotropic process has been connected with the geometrical problem of close packing of hyperspheres, whose known solution up to the eighth dimension allows the explicit specification of the most efficient sampling lattices. Second, a set of isotropic weighting functions has been derived which, although lacking the orthogonality property of the canonical functions, are relatively simple to calculate and instrument. A general formula is given and the second, third, and fourth dimensional functions calculated.

The sampling theorem is found to be readily adaptable to the interpolation of homogeneous multidimensional stochastic processes. The general optimum (mean-square) post-sampling filter for nonwave-num-

ber-limited processes was incidentally derived in the course of proving that wave-number-limited processes may be reproduced with zero mean-square error from samples taken over a lattice with suitably small repetition vectors.

Finally, the problem of optimum prefiltering of multidimensional data, for sampling on a lattice of specified density, was examined. It was found that the optimum operation (yielding minimum mean-square error *uniformly averaged* over sampling space) consists of ideal wave-number limiting within a cell corresponding to the given sampling lattice. This relationship is the ultimate justification for the study of admittedly artificial "band-limited" processes and allows the establishment of lower and upper bounds on the average mean-square error of *optimally reconstructed* sampled data: respectively, one and two times the total spectral intensity outside the most favorable wave-number cell within the constraint of repeatability corresponding to the given sampling lattice.

The authors recognize that the work presented here has barely touched upon a vast array of problems involving multidimensional sampling, filtering, and information handling. Questions of noise, limited data spaces, performance criteria other than mean-square and uniform averaging, vector processes, and the relationship of time and displacement correlation to the applicable dynamic equations, remain to be attacked. Finally, specific *system* design applications are needed in fields such as meteorology, oceanography, and optics—where constraints and tradeoffs such as filter realizability, lattice density in space and time, and sequential scanning, data transmission and processing, must be introduced. It is hoped that this paper will help to stimulate interest in these fields, where definitive results are urgently needed.

APPENDIX A. FOURIER SERIES EXPANSION OF PERIODIC DELTA FUNCTIONS

Let there be defined a periodic lattice of Dirac delta functions in N-dimensional Euclidean space:

$$\Delta(\mathbf{x}) = \sum_{[l]} \delta(\mathbf{x} - \mathbf{v}_{[l]}), \tag{A.1}$$

where the vectors $\{\mathbf{v}_j\}$ form a basis for the space.

The N-dimensional Fourier series expansion of a periodic function $H(\mathbf{x})$ is defined as

$$H(\mathbf{x}) = \sum_{[m]} C_{[m]} e^{i\mathbf{x}\,\mathbf{u}_{[m]}}, \tag{A.2}$$

with the periodicity of $H(\mathbf{x})$ expressed by

$$H(\mathbf{x} + \mathbf{v}_{[i]}) = H(\mathbf{x}), \tag{A.3}$$

provided that the "periodicity" vectors $\{\mathbf{v}_j\}$ are related to the "wave-number" vectors $\{\mathbf{u}_k\}$ by

$$\mathbf{v}_j \cdot \mathbf{u}_k = 2\pi\delta_{jk}\,. \tag{A.4}$$

The coefficients in the expansion (A.2) are determined from the integral

$$C_{[m]} = \frac{1}{Q}\int_{\text{Б}} H(\mathbf{x}) e^{-i\mathbf{x}\cdot\mathbf{u}_{[m]}}\, d\mathbf{x}, \tag{A.5}$$

where Б is the parallelepiped of hypervolume Q whose edges are the basis vectors $\{\mathbf{v}_j\}$. This result follows immediately if we can demonstrate that the exponential expansion functions in (A.2) are orthogonal over the parallelepiped Б, i.e.,

$$\int_{\text{Б}} e^{-i\mathbf{x}\cdot\mathbf{u}_{[k]}}\, d\mathbf{x} = \left\{\begin{array}{ll} Q, & k_1 = k_2 = \cdots = k_N = 0 \\ 0, & k_1, k_2, \cdots, k_N = 0, \pm 1, \pm 2, \cdots \\ & (\text{except } k_1 = k_2 = \cdots = k_N = 0) \end{array}\right\}. \tag{A.6}$$

To do this, we transform the integral (A.6) from X space to Λ space by the relation

$$\mathbf{x} = \lambda_1\mathbf{v}_1 + \lambda_2\mathbf{v}_2 + \cdots + \lambda_N\mathbf{v}_N\,, \qquad 0 \leqq \lambda_j < 1, \tag{A.7}$$

the Jacobian being a constant defined as Q:

$$Q = \begin{vmatrix} v_{11} & v_{21} & \cdots & v_{N1} \\ v_{12} & v_{22} & & \vdots \\ \vdots & & \ddots & \\ v_{1N} & & & v_{NN} \end{vmatrix}. \tag{A.8}$$

Now using the relations (A.4), the multiple integral becomes separable:

$$\begin{aligned} \int_{\text{Б}} e^{-i\mathbf{x}\cdot\mathbf{u}_{[k]}}\, d\mathbf{x} &= Q\int_0^1 \cdots \int_0^1 e^{-i2\pi(k_1\lambda_1 + k_2\lambda_2 + \cdots + k_N\lambda_N)}\, d\lambda_1\, d\lambda_2 \cdots d\lambda_N \\ &= Q\prod_{j=1}^{N}\int_0^1 e^{-i2\pi k_j\lambda_j}\, d\lambda_j \\ &= \left\{\begin{array}{ll} Q, & k_1 = k_2 = \cdots = k_N = 0 \\ 0, & k_1, k_2, \cdots, k_N = 0, \pm 1, \pm 2, \cdots \\ & (\text{except } k_1 = k_2 = \cdots = k_N = 0) \end{array}\right\}. \end{aligned} \tag{A.9}$$

By substituting $k_1 = k_2 = \cdots = k_N = 0$ on the left side of (A.9), we see that Q is simply the volume of the parallelepiped Б. It is evident that Б contains one and only one point of the lattice in X space.

Now expanding $\Delta(\mathbf{x})$ in Fourier series, and noting that only one delta impulse occurs within Б (i.e., at the origin), we compute the coefficients from (A.5):

$$\begin{aligned} C_{[m]} &= \frac{1}{Q} \int_{\text{Б}} \delta(\mathbf{x}) e^{-i\mathbf{x}\cdot\mathbf{u}_{[m]}} \, d\mathbf{x} \\ &= \frac{1}{Q} . \end{aligned} \tag{A.10}$$

Therefore, we have

$$\Delta(\mathbf{x}) = \sum_{[m]} \frac{1}{Q} e^{i\mathbf{x}\cdot\mathbf{u}_{[m]}} . \tag{A.11}$$

APPENDIX B. RELATIONSHIP BETWEEN HYPERVOLUMES IN SAMPLING AND WAVE-NUMBER SPACES

Given a parallelepiped in N-dimensional sampling space X, defined by its edge vectors $\{\mathbf{v}_j\}$ $(j = 1, 2, \cdots, N)$ and having hypervolume Q, we define a set of vectors $\{\mathbf{u}_k\}$ $(k = 1, 2, \cdots, N)$ in wave-number space Ω such that

$$\mathbf{v}_j \cdot \mathbf{u}_k = 2\pi\delta_{jk} , \tag{B.1}$$

where δ_{jk} is Kronecker's delta. We wish to find the hypervolume P of the parallelepiped in wave-number space defined by the edge vectors $\{\mathbf{u}_k\}$.

We transform the volume integral in both spaces to an integral over a unit cube by the linear relations

$$\begin{aligned} \mathbf{x} &= \sigma_1\mathbf{v}_1 + \sigma_2\mathbf{v}_2 + \cdots + \sigma_N\mathbf{v}_N , \qquad (0 \leqq \sigma_j \leqq 1); \\ \boldsymbol{\omega} &= \rho_1\mathbf{u}_1 + \rho_2\mathbf{u}_2 + \cdots + \rho_N\mathbf{u}_N , \qquad (0 \leqq \rho_k \leqq 1). \end{aligned} \tag{B.2}$$

In each case the Jacobian of the transformation is simply the original volume; thus we have

$$Q = \begin{vmatrix} v_{11} & v_{21} & \cdots & v_{N1} \\ v_{12} & v_{22} & & \vdots \\ \vdots & & \ddots & \\ v_{1N} & \cdots & & v_{NN} \end{vmatrix} ; \quad P = \begin{vmatrix} u_{11} & u_{21} & \cdots & u_{N1} \\ u_{12} & u_{22} & & \vdots \\ \vdots & & \ddots & \\ u_{1N} & \cdots & & u_{NN} \end{vmatrix} . \tag{B.3}$$

But since a determinant is unchanged by transposition (Hildebrand,

1952), we also have

$$P = \begin{vmatrix} u_{11} & u_{12} & \cdots & u_{1N} \\ u_{21} & u_{22} & & \vdots \\ \vdots & & \ddots & \\ u_{N1} & \cdots & & u_{NN} \end{vmatrix} . \tag{B.4}$$

Now considering the matrices corresponding to these determinants, and using the relations (B.1), we see that

$$\tilde{\mathbf{P}}\mathbf{Q} = \begin{bmatrix} 2\pi & 0 & \cdots & 0 \\ 0 & 2\pi & & \vdots \\ \vdots & & \ddots & \\ 0 & \cdots & & 2\pi \end{bmatrix} = 2\pi\mathbf{I}. \tag{B.5}$$

But (Hildebrand, 1952)

$$PQ = \det \mathbf{P} \det \mathbf{Q} = \det \tilde{\mathbf{P}} \det \mathbf{Q} = \det \tilde{\mathbf{P}}\mathbf{Q} = (2\pi)^N. \tag{B.6}$$

Therefore, as we wished to show,

$$P = \frac{(2\pi)^N}{Q} . \tag{B.7}$$

APPENDIX C. SAMPLING LATTICES FOR N-DIMENSIONAL ISOTROPIC FUNCTIONS

The problem of closest packing of hyperspheres in Euclidean N-space has attracted the attention of a number of geometers. Coxeter (1951) has shown that the lattice of centers in the configuration of closest packing is defined by an associated "extreme quadratic form". These forms have been determined up to eight-dimensional spaces.

Coxeter's extreme quadratic forms may be expressed as

$$\sum_{i=1}^{N} \sum_{j=1}^{N} \alpha_{ij} x_i x_j , \tag{C.1}$$

in which the α_{ij} are the inner products of the vectors defining the lattice of centers of close-packed spheres. In our notation,

$$\alpha_{ij} = \mathbf{u}_i \cdot \mathbf{u}_j . \tag{C.2}$$

To adapt these results to our present purposes, we first write the symmetrical matrix $[\alpha_{ij}]$ as obtained directly from Coxeter's quadratic forms. Next, a particular set of vectors $\{\mathbf{u}_i\}$ is selected by choosing arbitrarily the vector $\mathbf{u}_1$. Normally, this would involve the solution of simultaneous

quadratic equations; however, the simplicity of the $[\alpha_{ij}]$ matrix allows the $\{\mathbf{u}_i\}$ vectors to be written by inspection. The set is, of course, not unique, since rotational transformation does not change the inner products. The $\{\mathbf{u}_i\}$ vectors are written in matrix form $[u_{ji}]$ with the components of the ith vector lying in the ith column. Then, from the $[u_{ji}]$ matrix, the normalized $[v_{ji}]$ matrix, exhibiting the $\{\mathbf{v}_i\}$ vectors in column form, is simply written as the transposed inverse. These results are summarized in Table C.I.

TABLE C.I

ISOTROPIC SAMPLING AND WAVE-NUMBER LATTICES

1

$$[a_{ij}] = [1] \qquad [u_{ji}] = [1] \qquad [v_{ji}] = [1]$$

$$Q = \frac{1}{2B} \qquad R = 4\pi B$$

2

$$[a_{ij}] = \begin{bmatrix} 1 & -\frac{1}{2} \\ -\frac{1}{2} & 1 \end{bmatrix} \qquad [u_{ji}] = \begin{bmatrix} \frac{\sqrt{3}}{2} & 0 \\ -\frac{1}{2} & 1 \end{bmatrix} \qquad [v_{ji}] = \begin{bmatrix} \frac{2}{\sqrt{3}} & \frac{1}{\sqrt{3}} \\ 0 & 1 \end{bmatrix}$$

$$Q = \frac{1}{2\sqrt{3}\,B^2} \qquad R = 4\pi^3 B^2$$

3

$$[a_{ij}] = \begin{bmatrix} 1 & -\frac{1}{2} & 0 \\ -\frac{1}{2} & 1 & -\frac{1}{2} \\ 0 & -\frac{1}{2} & 1 \end{bmatrix} \qquad [u_{ji}] = \begin{bmatrix} \frac{1}{\sqrt{2}} & -\frac{1}{\sqrt{2}} & \frac{1}{\sqrt{2}} \\ \frac{1}{\sqrt{2}} & 0 & -\frac{1}{\sqrt{2}} \\ 0 & \frac{1}{\sqrt{2}} & 0 \end{bmatrix} \qquad [v_{ji}] = \begin{bmatrix} \frac{1}{\sqrt{2}} & 0 & \frac{1}{\sqrt{2}} \\ \frac{1}{\sqrt{2}} & 0 & -\frac{1}{\sqrt{2}} \\ \frac{1}{\sqrt{2}} & \sqrt{2} & \frac{1}{\sqrt{2}} \end{bmatrix}$$

$$Q = \frac{1}{4\sqrt{2}\,B^3} \qquad R = \frac{32}{3}\pi^4 B^3$$

4

$$[a_{ij}] = \begin{bmatrix} 1 & -\frac{1}{2} & 0 & 0 \\ -\frac{1}{2} & 1 & -\frac{1}{2} & -\frac{1}{2} \\ 0 & -\frac{1}{2} & 1 & 0 \\ 0 & -\frac{1}{2} & 0 & 1 \end{bmatrix} \qquad [u_{ji}] = \begin{bmatrix} 1 & -\frac{1}{2} & 0 & 0 \\ 0 & \frac{1}{2} & 0 & 0 \\ 0 & -\frac{1}{2} & 1 & 0 \\ 0 & -\frac{1}{2} & 0 & 1 \end{bmatrix} \qquad [v_{ji}] = \begin{bmatrix} 1 & 0 & 0 & 0 \\ 1 & 2 & 1 & 1 \\ 0 & 0 & 1 & 0 \\ 0 & 0 & 0 & 1 \end{bmatrix}$$

$$Q = \frac{1}{8B^4} \qquad R = 8\pi^6 B^4$$

5

$$[a_{ij}] = \begin{bmatrix} 1 & -\frac{1}{2} & 0 & 0 & 0 \\ -\frac{1}{2} & 1 & -\frac{1}{2} & 0 & 0 \\ 0 & -\frac{1}{2} & 1 & -\frac{1}{2} & -\frac{1}{2} \\ 0 & 0 & -\frac{1}{2} & 1 & 0 \\ 0 & 0 & -\frac{1}{2} & 0 & 1 \end{bmatrix} \qquad [u_{ji}] = \begin{bmatrix} 1 & -\frac{1}{2} & 0 & 0 & 0 \\ 0 & -\frac{1}{\sqrt{2}} & \frac{1}{\sqrt{2}} & 0 & 0 \\ 0 & \frac{1}{2} & 0 & 0 & 0 \\ 0 & 0 & -\frac{1}{2} & 1 & 0 \\ 0 & 0 & -\frac{1}{2} & 0 & 1 \end{bmatrix}$$

$$[v_{ji}] = \begin{bmatrix} 1 & 0 & 0 & 0 & 0 \\ 0 & 0 & \sqrt{2} & \frac{1}{\sqrt{2}} & \frac{1}{\sqrt{2}} \\ 1 & 2 & 2 & 1 & 1 \\ 0 & 0 & 0 & 1 & 0 \\ 0 & 0 & 0 & 0 & 1 \end{bmatrix}$$

$$Q = \frac{1}{8\sqrt{2}\,B^5}$$

$$R = \frac{256}{15}\pi^7 B^5$$

TABLE C.I (continued)

6

$$[a_{ij}] = \begin{bmatrix} 1 & -\frac{1}{2} & 0 & 0 & 0 & 0 \\ -\frac{1}{2} & 1 & -\frac{1}{2} & 0 & 0 & 0 \\ 0 & -\frac{1}{2} & 1 & -\frac{1}{2} & 0 & -\frac{1}{2} \\ 0 & 0 & -\frac{1}{2} & 1 & -\frac{1}{2} & 0 \\ 0 & 0 & 0 & -\frac{1}{2} & 1 & 0 \\ 0 & 0 & -\frac{1}{2} & 0 & 0 & 1 \end{bmatrix} \qquad [u_{ji}] = \begin{bmatrix} 1 & -\frac{1}{2} & 0 & 0 & 0 & 0 \\ 0 & \frac{1}{\sqrt{2}} & \frac{1}{\sqrt{2}} & 0 & -\frac{1}{2\sqrt{2}} & 0 \\ 0 & \frac{1}{2} & 0 & 0 & -\frac{1}{2} & 0 \\ 0 & 0 & 0 & 0 & \frac{\sqrt{3}}{2\sqrt{2}} & 0 \\ 0 & 0 & -\frac{1}{2} & 1 & -\frac{1}{2} & 0 \\ 0 & 0 & -\frac{1}{2} & 0 & 0 & 1 \end{bmatrix}$$

$$[v_{ji}] = \begin{bmatrix} 1 & 0 & 0 & 0 & 0 & 0 \\ 0 & 0 & \sqrt{2} & \frac{1}{\sqrt{2}} & 0 & \frac{1}{\sqrt{2}} \\ 1 & 2 & 2 & 1 & 0 & 1 \\ \frac{\sqrt{2}}{\sqrt{3}} & \frac{2\sqrt{2}}{\sqrt{3}} & \sqrt{6} & \frac{\sqrt{3}}{\sqrt{2}} & \frac{2\sqrt{2}}{\sqrt{3}} & \frac{\sqrt{3}}{\sqrt{2}} \\ 0 & 0 & 0 & 1 & 0 & 0 \\ 0 & 0 & 0 & 0 & 0 & 1 \end{bmatrix}$$

$$Q = \frac{1}{8\sqrt{3}\,B^6}$$

$$R = \frac{32}{3}\pi^9 B^6$$

7

$$[a_{ij}] = \begin{bmatrix} 1 & -\frac{1}{2} & 0 & 0 & 0 & 0 & 0 \\ -\frac{1}{2} & 1 & -\frac{1}{2} & 0 & 0 & 0 & 0 \\ 0 & -\frac{1}{2} & 1 & -\frac{1}{2} & 0 & 0 & 0 \\ 0 & 0 & -\frac{1}{2} & 1 & -\frac{1}{2} & 0 & -\frac{1}{2} \\ 0 & 0 & 0 & -\frac{1}{2} & 1 & -\frac{1}{2} & 0 \\ 0 & 0 & 0 & 0 & -\frac{1}{2} & 1 & 0 \\ 0 & 0 & 0 & -\frac{1}{2} & 0 & 0 & 1 \end{bmatrix} \qquad [u_{ji}] = \begin{bmatrix} 1 & -\frac{1}{2} & 0 & 0 & 0 & 0 & 0 \\ 0 & -\frac{1}{2} & 1 & -\frac{1}{2} & 0 & 0 & 0 \\ 0 & \frac{1}{\sqrt{2}} & 0 & -\frac{1}{2\sqrt{2}} & 0 & 0 & 0 \\ 0 & 0 & 0 & \frac{\sqrt{3}}{2\sqrt{2}} & \frac{\sqrt{2}}{\sqrt{3}} & 0 & 0 \\ 0 & 0 & 0 & 0 & \frac{1}{2\sqrt{3}} & 0 & 0 \\ 0 & 0 & 0 & 0 & -\frac{1}{2} & 1 & 0 \\ 0 & 0 & 0 & -\frac{1}{2} & 0 & 0 & 1 \end{bmatrix}$$

$$[v_{ji}] = \begin{bmatrix} 1 & 0 & 0 & 0 & 0 & 0 & 0 \\ 0 & 0 & 1 & 0 & 0 & 0 & 0 \\ \frac{1}{\sqrt{2}} & \sqrt{2} & \frac{1}{\sqrt{2}} & 0 & 0 & 0 & 0 \\ \frac{1}{\sqrt{6}} & \frac{\sqrt{2}}{\sqrt{3}} & \frac{\sqrt{3}}{\sqrt{2}} & \frac{2\sqrt{2}}{\sqrt{3}} & 0 & 0 & \frac{\sqrt{2}}{\sqrt{3}} \\ \frac{2}{\sqrt{3}} & \frac{4}{\sqrt{3}} & 2\sqrt{3} & \frac{3}{\sqrt{3}} & 2\sqrt{3} & \sqrt{3} & \frac{4}{\sqrt{3}} \\ 0 & 0 & 0 & 0 & 0 & 1 & 0 \\ 0 & 0 & 0 & 0 & 0 & 0 & 1 \end{bmatrix}$$

$$Q = \frac{1}{16B^7}$$

$$R = \frac{2048}{105}\pi^{10}B^7$$

Coxeter's forms are normalized to a sphere radius of one-half unit. To obtain the sampling lattice for a wave-number cutoff of $2\pi B$ radians per unit distance, the $\{\mathbf{u}_i\}$ vectors shown must be multiplied by $4\pi B$, while the $\{\mathbf{v}_i\}$ vectors are to be divided by $2B$.

Table C.I also lists, for reference, the quantity Q_N [the determinant of the $[v_{ji}]$ matrix divided by $(2B)^N$] as well as R (the volume of a hypersphere of radius $2\pi B$). These are later used in calculating the efficiencies of various sampling plans.

In Table C.II we list the maximum achievable sampling efficiency for isotropic functions in the space of given dimensionality. For reference, the efficiency of the largest simple cubic lattice yielding exact reproduction is also listed.

TABLE C.I (continued)

8

$$[a_{ij}] = \begin{bmatrix} 1 & -\frac{1}{2} & 0 & 0 & 0 & 0 & 0 & 0 \\ -\frac{1}{2} & 1 & -\frac{1}{2} & 0 & 0 & 0 & 0 & 0 \\ 0 & -\frac{1}{2} & 1 & -\frac{1}{2} & 0 & 0 & 0 & 0 \\ 0 & 0 & -\frac{1}{2} & 1 & -\frac{1}{2} & 0 & 0 & 0 \\ 0 & 0 & 0 & -\frac{1}{2} & 1 & -\frac{1}{2} & 0 & -\frac{1}{2} \\ 0 & 0 & 0 & 0 & -\frac{1}{2} & 1 & -\frac{1}{2} & 0 \\ 0 & 0 & 0 & 0 & 0 & -\frac{1}{2} & 1 & 0 \\ 0 & 0 & 0 & 0 & -\frac{1}{2} & 0 & 0 & 1 \end{bmatrix} \qquad [u_{ji}] = \begin{bmatrix} 1 & -\frac{1}{2} & 0 & 0 & 0 & 0 & 0 & 0 \\ 0 & -\frac{1}{2} & 1 & -\frac{1}{2} & 0 & 0 & 0 & 0 \\ 0 & \frac{1}{\sqrt{2}} & 0 & \frac{1}{2\sqrt{2}} & 0 & 0 & 0 & 0 \\ 0 & 0 & 0 & \frac{\sqrt{5}}{2\sqrt{2}} & \frac{\sqrt{2}}{\sqrt{5}} & 0 & 0 & 0 \\ 0 & 0 & 0 & 0 & \frac{\sqrt{7}}{2\sqrt{2}} & \frac{\sqrt{5}}{\sqrt{7}} & 0 & 0 \\ 0 & 0 & 0 & 0 & 0 & \frac{1}{2\sqrt{7}} & 0 & 0 \\ 0 & 0 & 0 & 0 & 0 & 0 & \frac{1}{2\sqrt{7}} & 1 & 0 \\ 0 & 0 & 0 & 0 & 0 & -\frac{1}{2} & 0 & 0 & 1 \end{bmatrix}$$

$$[v_{ji}] = \begin{bmatrix} 1 & 0 & 0 & 0 & 0 & 0 & 0 & 0 \\ 0 & 0 & 1 & 0 & 0 & 0 & 0 & 0 \\ \frac{1}{\sqrt{2}} & \sqrt{2} & \frac{1}{\sqrt{2}} & 0 & 0 & 0 & 0 & 0 \\ \frac{1}{\sqrt{10}} & \frac{\sqrt{2}}{\sqrt{5}} & \frac{3}{\sqrt{10}} & \frac{2\sqrt{2}}{\sqrt{5}} & 0 & 0 & 0 & 0 \\ \frac{2}{\sqrt{35}} & \frac{4}{\sqrt{35}} & \frac{6}{\sqrt{35}} & \frac{8}{\sqrt{35}} & \frac{2\sqrt{5}}{\sqrt{7}} & 0 & 0 & \frac{\sqrt{5}}{\sqrt{7}} \\ \frac{4}{\sqrt{7}} & \frac{8}{\sqrt{7}} & \frac{12}{\sqrt{7}} & \frac{16}{\sqrt{7}} & \frac{20}{\sqrt{7}} & 2\sqrt{7}\sqrt{7} & \frac{10}{\sqrt{7}} & \\ 0 & 0 & 0 & 0 & 0 & 0 & 1 & 0 \\ 0 & 0 & 0 & 0 & 0 & 0 & 0 & 1 \end{bmatrix}$$

$$Q = \frac{1}{16\,B^8}$$

$$R = \frac{32}{3}\pi^{11}B^8$$

TABLE C.II

ISOTROPIC SAMPLING EFFICIENCY

Dimensionality	Maximum sampling efficiency (%)	Efficiency of cubic lattice (%)
1	100.	100.
2	90.8	78.5
3	74.2	52.3
4	61.7	30.8
5	46.6	16.45
6	37.3	8.08
7	29.5	3.69
8	8.08	0.504

In addition to the two- and three-dimensional lattices appearing in Tables C.I and C.II, Miyakawa (1959) also calculated the efficiencies of a face-centered cubic lattice (67.8%) and of a regular hexagonal lattice (60.3%) for sampling a three-dimensional isotropic function. These, as expected, are intermediate in efficiency between the simple cubic lattice and the optimum body-centered cubic lattice.

APPENDIX D. PROOF OF THE ORTHOGONALITY PROPERTY FOR CANONICAL SAMPLING FUNCTIONS

Consider a spectral function $G_c(\omega)$ which is a constant Q over a repeatable cell in wave-number space (as illustrated in Fig. 4), and which

vanishes elsewhere. Then its inverse Fourier transform $g_c(\mathbf{x})$ has the property

$$g_c(l_1\mathbf{v}_1 + l_2\mathbf{v}_2 + \cdots + l_N\mathbf{v}_N) = \begin{cases} 1, & l_1 = l_2 = \cdots = l_N = 0 \\ 0, & l_1, l_2, \cdots, l_N = 0, \pm 1, \pm 2, \cdots \\ & (\text{except } l_1 = l_2 = \cdots = l_N = 0) \end{cases}, \tag{D.1}$$

where the vectors $\{\mathbf{v}_j\}$ are related to the spectrum repetition vectors $\{\mathbf{u}_k\}$ through the conditions

$$\mathbf{v}_j \cdot \mathbf{u}_k = 2\pi\delta_{jk} . \tag{D.2}$$

The constant Q is the hypervolume of the parallelepiped whose edges are the vectors $\{\mathbf{v}_j\}$, and δ_{jk} is Kronecker's delta.

To demonstrate the above assertion, it is first necessary to define the term "repeatable cell": a repeatable cell on the vector basis $\{\mathbf{u}_k\}$ is a measurable region which contains one and only one image of every point in the space, an image being defined as the position of the point when translated by a vector

$$\begin{aligned} &\mathbf{u}_{[m]} = m_1\mathbf{u}_1 + m_2\mathbf{u}_2 + \cdots + m_N\mathbf{u}_N ; \\ &m_1, m_2, \cdots, m_N = 0, \pm 1, \pm 2, \cdots . \end{aligned} \tag{D.3}$$

The inverse transform of $G_c(\boldsymbol{\omega})$ is thus

$$g_c(\mathbf{x}) = \frac{Q}{(2\pi)^N} \int_{[\text{repeatable cell}]} e^{i\boldsymbol{\omega}\cdot\mathbf{x}}\, d\boldsymbol{\omega}, \tag{D.4}$$

and, at the sampling points

$$\begin{aligned} g_c(\mathbf{v}_{[l]}) &= g_c(l_1\mathbf{v}_1 + l_2\mathbf{v}_2 + \cdots + l_N\mathbf{v}_N) \\ &= \frac{Q}{(2\pi)^N} \int_{[\text{repeatable cell}]} \exp\left[i\boldsymbol{\omega}\cdot(l_1\mathbf{v}_1 + l_2\mathbf{v}_2 + \cdots + l_N\mathbf{v}_N)\right] d\boldsymbol{\omega}. \end{aligned} \tag{D.5}$$

We now note that

$$\begin{aligned} &\exp\left[i(\boldsymbol{\omega} + m_1\mathbf{u}_1 + \cdots + m_N\mathbf{u}_N)\cdot(l_1\mathbf{v}_1 + \cdots + l_N\mathbf{v}_N)\right] \\ &\qquad = \exp\left[i\boldsymbol{\omega}\cdot(l_1\mathbf{v}_1 + \cdots + l_N\mathbf{v}_N)\right] \end{aligned} \tag{D.6}$$

for all integral values of m_k and l_j. Thus, for these values of $\mathbf{x}$, the integrals over all repeatable cells with the same vector basis $\{\mathbf{u}_k\}$ are equal,

and we may replace the original region of integration with a parallelepiped whose edges are the vectors $\{\mathbf{u}_k\}$. This, however, makes (D.5) equivalent, except for a constant factor and the dummy variable, to (A.6) which is shown in Appendix A to vanish for all integral values of the coefficients l_j except when all are zero. When all coefficients l_j vanish, Appendix B shows that the integral in (D.5) equals $\frac{(2\pi)^N}{Q}$, so that in this case $g_c(\mathbf{0}) = 1$, as was to be proved.

The usual definition of orthogonality, viz.,

$$\frac{1}{Q}\int_X g_c(\mathbf{x} - \mathbf{v}_{[m]})\hat{g}_c(\mathbf{x} - \mathbf{v}_{[l]})\,d\mathbf{x} = \delta_{[m]}^{[l]} = \begin{cases} 1, & [l] = [m] \\ 0, & [l] \neq [m] \end{cases}, \quad \text{(D.7)}$$

where $\hat{}$ denotes the complex conjugate, follows immediately from the above upon application of the Parseval relation:

$$\begin{aligned} &\frac{1}{Q}\int_X g_c(\mathbf{x} - \mathbf{v}_{[m]})\hat{g}_c(\mathbf{x} - \mathbf{v}_{[l]})\,d\mathbf{x} \\ &\quad = \frac{1}{(2\pi)^N Q}\int_\Omega G_c(\boldsymbol{\omega})\hat{G}_c(\boldsymbol{\omega})\exp\left[i\boldsymbol{\omega}\cdot(\mathbf{v}_{[l]} - \mathbf{v}_{[m]})\right]d\boldsymbol{\omega} \\ &\quad = \frac{Q}{(2\pi)^N}\int_{\text{[repeatable cell]}}\exp\left[i\boldsymbol{\omega}\cdot(\mathbf{v}_{[l]} - \mathbf{v}_{[m]})\right]d\boldsymbol{\omega} \\ &\quad = \delta_{[m]}^{[l]}\,. \end{aligned} \quad \text{(D.8)}$$

APPENDIX E. SIMULTANEOUS SOLUTION OF EQS. (46) AND (52)

A necessary condition for a minimum average mean-square error of a homogeneous process using both pre- and post-sampling filters is the simultaneous satisfaction of the following equations in the wave-number domain:

$$\Phi(\boldsymbol{\omega})\Gamma(-\boldsymbol{\omega}) = \frac{G(\boldsymbol{\omega})}{Q}\sum_{[m]}\Gamma(\boldsymbol{\omega} - \mathbf{u}_{[m]})\Gamma(\mathbf{u}_{[m]} - \boldsymbol{\omega})\Phi(\mathbf{u}_{[m]} - \boldsymbol{\omega}); \quad \text{(E.1)}$$

$$G(\boldsymbol{\omega}) = \frac{1}{Q}\sum_{[k]} G(\boldsymbol{\omega} + \mathbf{u}_{[k]})G(-\boldsymbol{\omega} - \mathbf{u}_{[k]})\Gamma(-\boldsymbol{\omega}). \quad \text{(E.2)}$$

We assume that $\Phi(\boldsymbol{\omega})$ is arbitrary and that it is everywhere nonvanishing. We will tentatively suppose $G(\boldsymbol{\omega})$ and $\Gamma(\boldsymbol{\omega})$ also to be nonvanishing and show that this leads to a contradiction. Solving (E.2) for $\Gamma(-\boldsymbol{\omega})$ and substituting in (E.1) yields

$$\Phi(\omega)\frac{QG(\omega)}{\sum_{[k]} G(\omega+\mathbf{u}_{[k]})G(-\omega-\mathbf{u}_{[k]})}$$

$$= \frac{G(\omega)}{Q}\sum_{[m]}\frac{QG(\mathbf{u}_{[m]}-\omega)}{\sum_{[l]} G(\mathbf{u}_{[m]}+\mathbf{u}_{[l]}-\omega)G(\omega-\mathbf{u}_{[m]}-\mathbf{u}_{[l]})} \tag{E.3}$$

$$\times \frac{QG(\omega-\mathbf{u}_{[m]})\Phi(\mathbf{u}_{[m]}-\omega)}{\sum_{[l]} G(\omega-\mathbf{u}_{[m]}+\mathbf{u}_{[l]})G(\mathbf{u}_{[m]}-\mathbf{u}_{[l]}-\omega)}.$$

Now changing variables in the summations of the right hand denominator by

$$\begin{aligned}\mathbf{u}_{[m]}+\mathbf{u}_{[l]} &= \mathbf{u}_{[r]}\,,\\ \mathbf{u}_{[l]}-\mathbf{u}_{[m]} &= \mathbf{u}_{[k]}\,,\end{aligned} \tag{E.4}$$

and noting the infinite limits of all summations, we obtain

$$\Phi(\omega) = \frac{\sum_{[m]} G(\omega-\mathbf{u}_{[m]})G(\mathbf{u}_{[m]}-\omega)\Phi(\mathbf{u}_{[m]}-\omega)}{\sum_{[r]} G(\omega-\mathbf{u}_{[r]})G(\mathbf{u}_{[r]}-\omega)}. \tag{E.5}$$

But examination of (E.5) reveals that $\Phi(\omega)$, which was assumed arbitrary and nonvanishing, is periodic on the lattice $\{\mathbf{u}_{[k]}\}$. Since this is a contradiction, $G(\omega)$, which was divided out of Eq. (E.3), cannot be everywhere nonvanishing.

We now prove the following statements:

1. $G(\omega)$ and $\Gamma(-\omega)$ take on zero or nonzero values simultaneously.

PROOF: From (E.1), $G(\omega) \neq 0$ if $\Gamma(-\omega) \neq 0$, and $\Gamma(-\omega) = 0$ if $G(\omega) = 0$. From (E.2), $\Gamma(-\omega) \neq 0$ if $G(\omega) \neq 0$, and $G(\omega) = 0$ if $\Gamma(-\omega) = 0$.

2. If $G(\omega) \neq 0$, then $G(\omega + \mathbf{u}_{[l]}) = 0$ for all $\mathbf{u}_{[l]} \neq 0$.

PROOF: From (E.2),

$$G(\omega+\mathbf{u}_{[l]})$$

$$= \frac{1}{Q}\sum_{[k]} G(\omega+\mathbf{u}_{[l]}+\mathbf{u}_{[k]})G(-\omega-\mathbf{u}_{[l]}-\mathbf{u}_{[k]})\Gamma(-\omega-\mathbf{u}_{[l]})$$

$$= \frac{1}{Q}\sum_{[m]} G(\omega+\mathbf{u}_{[m]})G(-\omega-\mathbf{u}_{[m]})\Gamma(-\omega-\mathbf{u}_{[l]})$$

$$= \frac{G(\omega)}{\Gamma(-\omega)}\Gamma(-\omega-\mathbf{u}_{[l]}),$$

and from (E.1),

$$\Phi(\omega + \mathbf{u}_{[l]})\Gamma(-\omega - \mathbf{u}_{[l]})$$

$$= \frac{G(\omega + \mathbf{u}_{[l]})}{Q} \sum_{[m]} \Gamma(\omega + \mathbf{u}_{[l]} - \mathbf{u}_{[m]}) \cdot \Gamma(\mathbf{u}_{[m]} - \omega - \mathbf{u}_{[l]})\Phi(\mathbf{u}_{[m]} - \omega - \mathbf{u}_{[l]})$$

$$= \frac{G(\omega + \mathbf{u}_{[l]})}{Q} \sum_{[k]} \Gamma(\omega - \mathbf{u}_{[k]})\Gamma(\mathbf{u}_{[k]} - \omega)\Phi(\mathbf{u}_{[k]} - \omega)$$

$$= G(\omega + \mathbf{u}_{[l]}) \frac{\Phi(\omega)\Gamma(-\omega)}{G(\omega)} = \Phi(\omega)\Gamma(-\omega - \mathbf{u}_{[l]}).$$

Therefore, if $\Gamma(-\omega - \mathbf{u}_{[l]}) \neq 0$, and consequently from *1* above $G(\omega + \mathbf{u}_{[l]}) \neq 0$, then $\Phi(\omega + \mathbf{u}_{[l]}) = \Phi(\omega)$. But since $\Phi(\omega)$ is arbitrary, this results in contradiction and therefore $G(\omega + \mathbf{u}_{[l]}) = 0$.

3. If $G(\omega) \neq 0$, then $G(-\omega) \neq 0$, and consequently $\Gamma(\omega) \neq 0$.

PROOF: From *2* above, (E.2) becomes

$$G(\omega) = \frac{1}{Q} G(\omega)G(-\omega)\Gamma(-\omega),$$

from which it is obvious that $G(-\omega) \neq 0$. The second part follows by change of variable, using *1*.

4. If $G(\omega) = 0$, then $G(-\omega) = 0$ and $\Gamma(\omega) = 0$.

PROOF: Change variables in *3* above.

5. Where $G(\omega) \neq 0$, $G(\omega)\Gamma(\omega) = Q$.

PROOF: Changing variable in (E.2) and dividing by $G(-\omega) \neq 0$, we obtain

$$1 = \frac{1}{Q} G(\omega)\Gamma(\omega).$$

Statements *1* to *5* above demonstrate that the functions $G(\omega)$ and $\Gamma(\omega)$ which simultaneously satisfy the necessary conditions (46) and (52) are nonvanishing and have a product Q over a region of wave-number space which is symmetrical with respect to the origin and lies wholly within a repeatable wave-number cell as defined in Appendix D. Both $G(\omega)$ and $\Gamma(\omega)$ vanish outside this region.

RECEIVED: June 29, 1962

REFERENCES

BALAKRISHNAN, A. V., (1957), A note on the sampling principle for continuous signals. *IRE Trans. on Information Theory* **IT-3**, 143–146.

BRACEWELL, R. N., (1956), Two dimensional aerial smoothing in radio astronomy. *Australian J. Phys.* **9,** 297–314.

BRILLOUIN, L., (1956), "Science and Information Theory," pp. 105–111. Academic Press, New York.

BROWN, W. M., (1961), Optimum prefiltering of sampled data. *IRE Trans. on Information Theory* **IT-7,** 269–270.

CHANG, S. S. L., (1961), Optimum transmission of continuous signal over a sampled data link. *AIEE Trans.* II **79,** 538–542.

COXETER, H. S. M., (1951), Extreme forms. *Can. J. Math.* **3,** 391–441.

DAVENPORT, W. B. JR., AND ROOT, W. L. (1958), "An Introduction to the Theory of Random Signals and Noise," pp. 96–101. McGraw-Hill, New York.

DERUSSO, P. M., (1961), Optimum linear filtering of signals prior to sampling. *AIEE Trans.* II **79,** 549–555.

ELIAS, P., (1955), Predictive coding. *IRE Trans. on Information Theory* **IT-1,** 16–33.

FOGEL, L. J., (1955), A note on the sampling theorem. *IRE Trans. on Information Theory* **IT-1,** 47–48.

HELMS, H. D., AND THOMAS, J. B., (1962), Truncation error of sampling theorem expansions. *Proc. IRE* **50,** 179–184.

HILDEBRAND, F. B., (1952), "Methods of Applied Mathematics," pp. 10–13. Prentice-Hall, Englewood Cliffs, N. J.

IGNAT'EV, N. K., (1960), On the discretization of signals with an unbounded spectrum. *Elektrosvyaz* **14,** 71–72.

JAGERMAN, D. L., AND FOGEL, L. J., (1956), Some general aspects of the sampling theorem. *IRE Trans. on Information Theory* **IT-2,** 139–146.

JAHNKE, E., AND EMDE, F. (1945), "Tables of Functions with Formulae and Curves," 4th ed., p. 151. Dover, New York.

JORDAN, K. L. JR., (1960), Discrete representations of random signals, pp. 122–124. Sc.D. thesis, MIT, Cambridge, Mass.

KOTEL'NIKOV, V. A., (1933), On the transmission capacity of "ether" and wire in electrocommunications. All-Union Energetics Committee, Izd. Red. Upr. Svyazi RKKA, Moscow.

LINDEN, D. A., AND ABRAMSON, N. M. (1960), A generalization of the sampling theorem. *Inform. and Control* **3,** 26–31.

MIDDLETON, D. (1960), "An Introduction to Statistical Communication Theory," pp. 206–212. McGraw-Hill, New York.

MIYAKAWA, H. (1959), Sampling theorem of stationary stochastic variables in multi-dimensional space. *J. Inst. Elec. Commun. Engrs. (Japan)* **42,** 421–427.

MORSE, P. M., AND FESHBACH, H. (1953), "Methods of Theoretical Physics," Part I, pp. 456–458. McGraw-Hill, New York.

NYQUIST, H. (1928), Certain topics in telegraph transmission theory. *Trans. AIEE* **47,** 617–644.

RAGAZZINI, J. R., AND FRANKLIN, G. F. (1958), "Sampled-Data Control Systems." McGraw-Hill, New York.

SASAKAWA, K. (1960, 1961), Application of Miyakawa's multi-dimensional sampling theorem. Papers published by Prof. Group on Inform. Theory, Inst. of

Elec. Commun. Engrs. of Japan. I—date unknown; II—September 30, 1960; III—date unknown; IV—June 24, 1961.

SHANNON, C. E. (1949), Communication in the presence of noise. *Proc. IRE* **37,** 10–21.

SHANNON, C. E., AND WEAVER, W. (1949), "The Mathematical Theory of Communication." Univ. of Illinois Press, Urbana, Ill.

SNEDDON, I. N. (1951), "Fourier Transforms," pp. 43–45. McGraw-Hill, New York.

SPILKER, J. J. JR. (1960), Theoretical bounds on the performance of sampled data communications systems. *IRE Trans. on Circuit Theory* **CT-7,** 335–341.

STEWART, R. M. (1956), Statistical design and evaluation of filters for the restoration of sampled data. *Proc. IRE* **44,** 253–258.

WHITTAKER, E. T. (1915), On the functions which are represented by the expansions of the interpolatory theory. *Proc. Roy. Soc. Edinburgh* **35,** 181–194.

ZHELEZNOV, N. A. (1958), The quantization of stochastic signals with infinite spectrum and some results of the theory of pulse transmission of information. *Radiotekh. i Elektron.* **3,** 3–18.